THE GEOLOGICAL SOCIETY OF AMERICA®

Emergence and evolution of Santa Maria Island (Azores)—The conundrum of uplifted islands revisited

Ricardo S. Ramalho[1,2,†], George Helffrich[3], José Madeira[4,5], Michael Cosca[6], Christine Thomas[7], Rui Quartau[5,8], Ana Hipólito[9], Alessio Rovere[10], Paul J. Hearty[11], and Sérgio P. Ávila[12,13]

[1]*School of Earth Sciences, University of Bristol, Wills Memorial Building, Queen's Road, Bristol, BS8 1RJ, UK*
[2]*Lamont-Doherty Earth Observatory at Columbia University, Comer Geochemistry Building, 61 Route 9W/P.O. Box 1000, Palisades, New York 10964-8000, USA*
[3]*Earth-Life Science Institute, Tokyo Institute of Technology, 2-12-1-IE-1 Ookayama, Meguro-ku, Tokyo, 152-8550, Japan*
[4]*Departamento de Geologia, Faculdade de Ciências, Universidade de Lisboa, 1749-016 Lisboa, Portugal*
[5]*Instituto Dom Luiz, Faculdade de Ciências, Universidade de Lisboa, 1749-016 Lisboa, Portugal*
[6]*U.S. Geological Survey, Denver Federal Center, MS 963, Denver, Colorado 80225, USA*
[7]*Institut für Geophysik, Westfälische Wilhelms-Universität, Corrensstraße 24, 48149 Münster, Germany*
[8]*Divisão de Geologia Marinha, Instituto Hidrográfico, Rua das Trinas, 49, 1249-093 Lisboa, Portugal*
[9]*Instituto de Investigação em Vulcanologia e Avaliação de Riscos (IVAR), Universidade dos Açores, Rua da Mãe de Deus, Edifício do Complexo Científico, 3º Andar-Ala Sul, 9500-321 Ponta Delgada, Açores, Portugal*
[10]*Center for Marine Environmental Sciences (MARUM), University of Bremen, and Leibniz Center for Tropical Marine Ecology (ZMT), Marum Pavillion 1110, 28359 Bremen, Germany*
[11]*Department of Environmental Studies, University of North Carolina, Wilmington, North Carolina 28403, USA*
[12]*Faculdade de Ciências da Universidade do Porto, Rua do Campo Alegre s/n, 4169-007 Porto, Portugal*
[13]*Centro de Investigação em Biodiversidade e Recursos Genéticos (CIBIO), InBIO Laboratório Associado, Pólo dos Açores, Departamento de Biologia da Universidade dos Açores, Campus de Ponta Delgada, Apartado 1422, 9501-801 Ponta Delgada, Açores, Portugal*

ABSTRACT

The growth and decay of ocean-island volcanoes are intrinsically linked to vertical movements. While the causes for subsidence are better understood, uplift mechanisms remain enigmatic. Santa Maria Island in the Azores Archipelago is an ocean-island volcano resting on top of young lithosphere, barely 480 km away from the Mid-Atlantic Ridge. Like most other Azorean islands, Santa Maria should be experiencing subsidence. Yet, several features indicate an uplift trend instead. In this paper, we reconstruct the evolutionary history of Santa Maria with respect to the timing and magnitude of its vertical movements, using detailed field work and $^{40}Ar/^{39}Ar$ geochronology. Our investigations revealed a complex evolutionary history spanning ~6 m.y., with subsidence up to ca. 3.5 Ma followed by uplift extending to the present day. The fact that an island located in young lithosphere experienced a pronounced uplift trend is remarkable and raises important questions concerning possible uplift mechanisms. Localized uplift in response to the tectonic regime affecting the southeastern tip of the Azores Plateau is unlikely, since the area is under transtension. Our analysis shows that the only viable mechanism able to explain the uplift is crustal thickening by basal intrusions, suggesting that intrusive processes play a significant role even on islands standing on young lithosphere, such as in the Azores.

INTRODUCTION

Ocean-island volcanoes are typically subjected to long-term subsidence, as the linear, age-progressive island chains of the Pacific Ocean clearly exemplify. This subsidence trend is essentially driven by mechanisms such as volcanic surface loading (Moore, 1970; Walcott, 1970; Menard, 1983), plate cooling with age (Parsons and Sclater, 1977; Stein and Stein, 1992), and hotspot swell decay (Morgan et al., 1995), all of which are influenced by fast plate movement away from the melting source. All these mechanisms (with perhaps the exception of hotspot swell decay) are reasonably well understood and are consistent within the plate tectonics and isostasy framework. In a similar fashion, within this fast-moving plate scenario, uplift episodes are easily explained by plate bending due to surface loading of younger islands further "upstream" along the chain (Walcott, 1970; Huppert et al., 2015), or by outer trench rise for islands approaching a subduction zone (Schmidt and Schmincke, 2000). A few island systems (e.g., the Cape Verdes, the Canaries, and Madeira Archipelago), however, fall out of pattern and feature numerous volcanic edifices that have experienced pronounced uplift trends, vertical stability, or complex uplift/subsidence histories (e.g., Staudigel and Schmincke, 1984; Klügel et al., 2005; Schmidt and Schmincke, 2002; Menéndez et al., 2008; Ramalho et al., 2010a, 2010b, 2010c, 2015; Madeira et al., 2010; Sepúlveda et al., 2015). These are mostly concentrated in, but not restricted to, the NE Atlantic, where the Nubian plate moves very slowly or is quasi-stationary with respect to the islands' melting source (Burke and Wilson, 1972; Ramalho et al., 2010b, 2015). The mechanisms behind such uplift trends or episodes, however, are still not completely understood and are the subject of ongoing debate, being the focus of the present study.

Several plausible mechanisms have been put forward to explain ocean-island uplift, all of which are likely to contribute in greater or lesser

†ric.ramalho@bristol.ac.uk

GSA Bulletin; March/April 2017; v. 129; no. 3/4; p. 372–391; doi: 10.1130/B31538.1; 7 figures; 1 table; Data Repository item 2016300; published online 21 October 2016.

For permission to copy, contact editing@geosociety.org
© 2016 Geological Society of America

degree to the observed uplift trends/episodes. For uplift acting at broad regional scale, hotspot swell growth by either spreading of melt residue or dynamic topography is regarded as the most plausible mechanism (Morgan et al., 1995; Zhong and Watts, 2002; Ramalho et al., 2010b; Wilson et al., 2010, Ramalho, 2011). At smaller regional scales, uplift may be generated by flexural uplift at the forebulge created by surface loading of nearby younger islands/seamounts (McNutt and Menard, 1978; Watts and ten Brink, 1989; Grigg and Jones, 1997; Huppert et al., 2015), by flexural uplift induced by subsurface loads ("underplating"; Watts and ten Brink, 1989; Ali et al., 2003), or by flexural rebound driven by mass wasting or erosion (Menard, 1983; Smith and Wessel, 2000; Menéndez et al., 2008). However, these uplift mechanisms still act upon a wide area (which largely depends on plate rheology) and thus cannot be used to explain contrasting uplift histories for edifices spatially close together (Ramalho et al., 2010a, 2010b, 2010c). Furthermore, surface loading has been shown to only generate uplift in the order of tens of meters (unless unrealistically thin elastic thicknesses are considered; McNutt and Menard, 1978). It also requires younger edifices being loaded at a suitable distance, and it fails to explain long-term uplift trends. In a similar fashion, significant uplift by erosive flexural rebound is problematic because it requires large volumes of eroded/mass wasted material, or because the effects of redistribution of wasted materials over wider areas need to be accounted for (Smith and Wessel, 2000). At local (island) scale, possibly only repeated intrusions at crustal and/or upper-mantle levels are capable of explaining pronounced, long-term uplift trends and episodes, as it has been proposed for slow-moving or quasi-stationary hotspot settings such as the Cape Verde, Madeira, and Canary Archipelagos (Klügel et al., 2005; Ramalho et al., 2010a, 2010b, 2010c, 2015; Madeira et al., 2010; Klügel et al., 2015). However, in order to gain a better insight into the origins of pronounced, long-term ocean-island uplift trends, further evidence is needed from different geodynamic settings, particularly from those where known uplift/subsidence models apply.

In this paper, we explore the enigmatic origins of ocean-island uplift using Santa Maria Island in the Azores Archipelago as a case study. Santa Maria is ~480 km away from the Mid-Atlantic Ridge (Fig. 1A) and rests on young lithosphere. Like most of the other Azorean islands, Santa Maria should therefore be experiencing long-term subsidence. However, it has long been recognized that this island must have experienced significant uplift due to the presence of raised marine terraces and the abundance of exposed marine volcanic and sedimentary sequences well above present sea level (Muecke et al., 1974; Serralheiro, 2003; Janssen et al., 2008; Ávila et al., 2012, 2015a; Meireles et al., 2013). Thus, Santa Maria is an ideal place in which to test competing models for the origins of ocean-island uplift. Here, we combine detailed field work and $^{40}Ar/^{39}Ar$ geochronology to track relative sea-level change throughout the island's lifetime in order to reconstruct the history of vertical movements affecting the island edifice. We then discuss the plausible mechanisms behind uplift, taking into account the geotectonic context in which the island is located. Thus, our study offers, for the first time, a detailed reconstruction of the evolutionary history of Santa Maria with respect to the magnitude and timing of its vertical movements and in relation to their possible origins.

GEOLOGICAL BACKGROUND

Santa Maria Island within the Azores Archipelago

The Azores Archipelago is a group of oceanic volcanic islands located in the mid–North Atlantic. The islands rise from a large, triangular-shaped bathymetric anomaly—the Azores Plateau, straddling the triple junction between the North American, Eurasian, and Nubian lithospheric plates (Fig. 1A; Lourenço et al., 1998; Gente et al., 2003; Miranda et al., 2017). Two of the Azorean islands, Flores and Corvo, sit west of the Mid-Atlantic Ridge, while the remaining seven islands sit to the east of the Mid-Atlantic Ridge, along the diffuse plate boundary between Eurasia and Nubia. The Azores are therefore situated in a complex tectonic setting, essen-

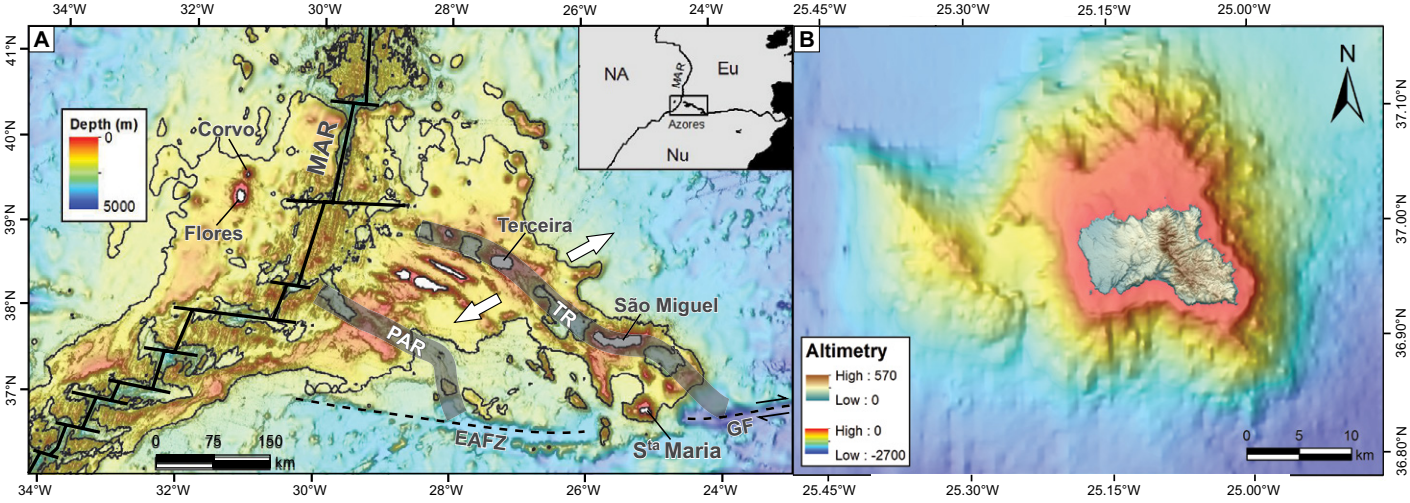

Figure 1. (A) Map illustrating the bathymetry and geotectonic setting of Santa Maria within the Azores triple junction. Santa Maria is located in the southeastern corner of the Azores Plateau, wedged in between the Terceira ultraslow-spreading ridge (TR), the dextral transcurrent Gloria fault (GF, part of the Azores-Gibraltar fault system), the currently inactive East Azores fault zone (EAFZ), and the early incipient Princess Alice Rift (PAR). White arrows represent the approximate spreading direction of TR. Upper-right inset depicts the regional setting of the Azores archipelago within the North American (NA), Eurasian (Eu), and Nubian (Nu) triple junction, and the Mid-Atlantic Ridge (MAR). (B) Bathymetry/altimetry of Santa Maria Island edifice. An extensive insular shelf lies to the north of the present-day island. Bathymetry on both subfigures was extracted from the EMODNET web portal (http://portal.emodnet-bathymetry.eu); subaerial topography was generated from a 1:5000 scale digital altimetric database.

tially governed by traction forces associated with seafloor spreading along the Mid-Atlantic Ridge, and right-lateral transtensional stress generated by movement between the Eurasian and Nubian plates (Madeira and Ribeiro, 1990; Madeira and Brum da Silveira, 2003; Vogt and Jung, 2004; Gente et al., 2003; Fernandes et al., 2006; Hipólito et al., 2013; Marques et al., 2013; Madeira et al., 2015; Miranda et al. 2015, 2017). The boundary between these two plates is diffuse, and deformation is presumably being accommodated along an ~140-km-wide shear zone of oblique extensional deformation bounded in the west by the Mid-Atlantic Ridge, in the north by the Terceira Rift, and fading out to the south along a line that connects the Mid-Atlantic Ridge to the Gloria fault, passing just south of Faial, Pico, and possibly Santa Maria (Marques et al., 2013; Hipólito et al., 2013). In the past, however, the Eurasian-Nubian plate boundary in the region probably was located further south, along the East Azores fault zone, a right-lateral transform fault that connected the Gloria fault with the Mid-Atlantic Ridge (Laughton and Whitmarsh, 1974; Searle, 1980; Madeira and Ribeiro, 1990; Luís et al., 1994; Luís and Miranda, 2008). The East Azores fault zone, however, seems to have become inactive sometime in the past, judging from its current lack of seismic activity (Krause and Watkins, 1970; Searle, 1980). The Azores triple junction (and consequently the Eurasian-Nubian plate boundary) therefore is inferred to have gradually migrated northward to its present position (Searle, 1980; Luís et al., 1994; Vogt and Jung, 2004; Luís and Miranda, 2008; Marques et al., 2013; Miranda et al., 2015, 2017). At an early stage (8–4 Ma), this transition took place through the development of the incipient Princess Alice Rift, followed by a ridge-jump to the more northerly Terceira Rift at ca. 4 Ma, eventually placing Santa Maria at the southern edge of the diffuse Eurasia-Nubia boundary (Miranda et al., 2015, 2017).

The excess magmatism that gave rise to the Azores Plateau and islands is generally thought to result from melting of anomalously hot and/or wet mantle (Schilling, 1975; Bonatti, 1990; Asimow et al., 2004; Beier et al., 2012; Beier et al., 2013; Métrich et al., 2014). In detail, however, the mechanism for this melting is still not well understood. Traditionally, Azorean magmatism has been viewed as resulting from a hotspot-ridge interaction, drawing excess heat from a mantle plume presently centered in the vicinity of Terceira Island (Gente et al., 2003; Madureira et al., 2005; Saki et al., 2015). Alternatively, magmatism has been attributed to the existence of a "wet spot" (Métrich et al., 2014), or to volatile-induced melting without involving a hot mantle plume (Schilling, 1975; Bonatti, 1990).

Santa Maria is the southeasternmost island in the Azores, sitting near the convergence among the Terceira Ridge, the Glória fault, and the East Azores fault zone (see Fig. 1A). The island is located on the eastern edge of the Azores Plateau, resting on lithosphere that is 47–49 m.y. old (Gente et al., 2003; Luís and Miranda, 2008; Miranda et al., 2015, 2017). Rising from the –2500 m isobath, Santa Maria's volcanic edifice presently reaches 587 m in elevation at Pico Alto, its highest point. Morphologically, the island edifice is extremely asymmetric, both above and below sea level (Fig. 1B). Below sea level, the insular shelf that surrounds the island is much wider and deeper on the northern side than on the other remaining sides. Effectively, the shelf edge in the north is at –120 m to –180 m and is located up to 6–7 km offshore (cf. Fig. 1B); in contrast, along the remaining sides, the same morphological feature can be found between –40 m and –80 m and usually extends less than 1.5 km offshore (Ávila et al., 2008). In a similar fashion, the island's topography is also asymmetric, featuring a stepped, west-sloping, low-relief plateau on the western (windward) side, in stark contrast with the higher, more mountainous eastern (leeward) portion of the edifice. Coastlines are typically high plunging cliffs, with rare small, perched sand/gravel beaches along protected bays (e.g., at Praia Formosa or at São Lourenço; Fig. 2A).

Santa Maria's Geological History

Santa Maria is the oldest island edifice in the Azores Archipelago, having emerged above sea level sometime during the late Miocene (Abdel-Monem et al., 1975; Féraud et al., 1980, 1981; Serralheiro et al., 1987; Storetvedt et al., 1989; Sibrant et al., 2015a). Based on previous studies (e.g., Agostinho, 1931; Zbyszewski and Ferreira, 1960; Serralheiro et al., 1987; Serralheiro and Madeira, 1990; Serralheiro, 2003; Ávila et al., 2012; Meireles et al., 2013; Sibrant et al., 2015a), and using the general stratigraphic scheme defined by Serralheiro et al. (1987) and Serralheiro (2003), the overall geological history of the island can be summarized (Fig. 2) as follows: (1) emergence of the volcanic edifice above sea level sometime during the late Miocene (the Cabrestantes and Porto Formations); (2) formation of a basaltic shield volcano during the late Miocene–early Pliocene (the Anjos volcanic complex); (3) subsequent truncation of the shield volcano by subaerial and marine erosion, with deposition of terrestrial and marine sediments and synchronous submarine volcanic activity on the eastern side of the island during the early Pliocene (the Touril volcano-sedimentary complex); (4) reemergence of the volcanic edifice by increased volcanic activity, initially exclusively submarine and later subaerial, forming a NNW-SSE–trending volcanic ridge during the early Pliocene (the Pico Alto volcanic complex); (5) erosion followed by low-volume posterosional volcanic activity, forming a set of monogenetic magmatic and hydromagmatic cones, and associated pyroclastic and effusive sequences, during the late Pliocene (the Feteiras Formation); and (6) uplift and erosion of the edifice from late Pliocene to the present. Sibrant et al. (2015a) also proposed a sequence of substantial flank collapses to the east, each at the end of the two main building stages of island evolution.

Despite the fact that Santa Maria's geological history is generally understood—and broadly constrained by the modern K/Ar geochronology data set of Sibrant et al. (2015a)—several key aspects in its evolutionary history remain to be clarified. The first and most important aspect concerns the magnitude, timing, and origins of its uplift/subsidence history, which have not been systematically studied. The second aspect is the precise timing of emergence for the first island edifice. Using K/Ar geochronology, Abdel-Monem et al. (1975), Féraud et al. (1980), and Féraud et al. (1981) suggested contrasting ages of ca. 8.12 and ca. 5.5 Ma, respectively, for the onset of subaerial volcanism, with the latter age bound being closer to the ca. 5.7 Ma recently reported by Sibrant et al. (2015a). However, neither of these studies attempted to date the hydromagmatic Cabrestantes Formation, which constitutes the seemingly oldest preserved evidence for island emergence (despite its very limited outcrop expression). Also, the stratigraphic/cartographic separation of the Feteiras Formation from the underlying Pico Alto volcanic complex is still poorly constrained, as Sibrant et al. (2015a) noted. Finally, so far, little is known about the precise, stratigraphically bound, geochemical evolution of the island edifice and its parental magmas. This paper aims to address the first two aspects, further contributing to our knowledge of Santa Maria's evolutionary history, and the geodynamic evolution of the Azores in general.

METHODOLOGY

Sampling of Uplift Tracers

The island's volcanostratigraphic succession was studied in detail to identify the highest position of relative sea level within each of the main stratigraphic units, and to gain insight on the overall evolutionary history of the

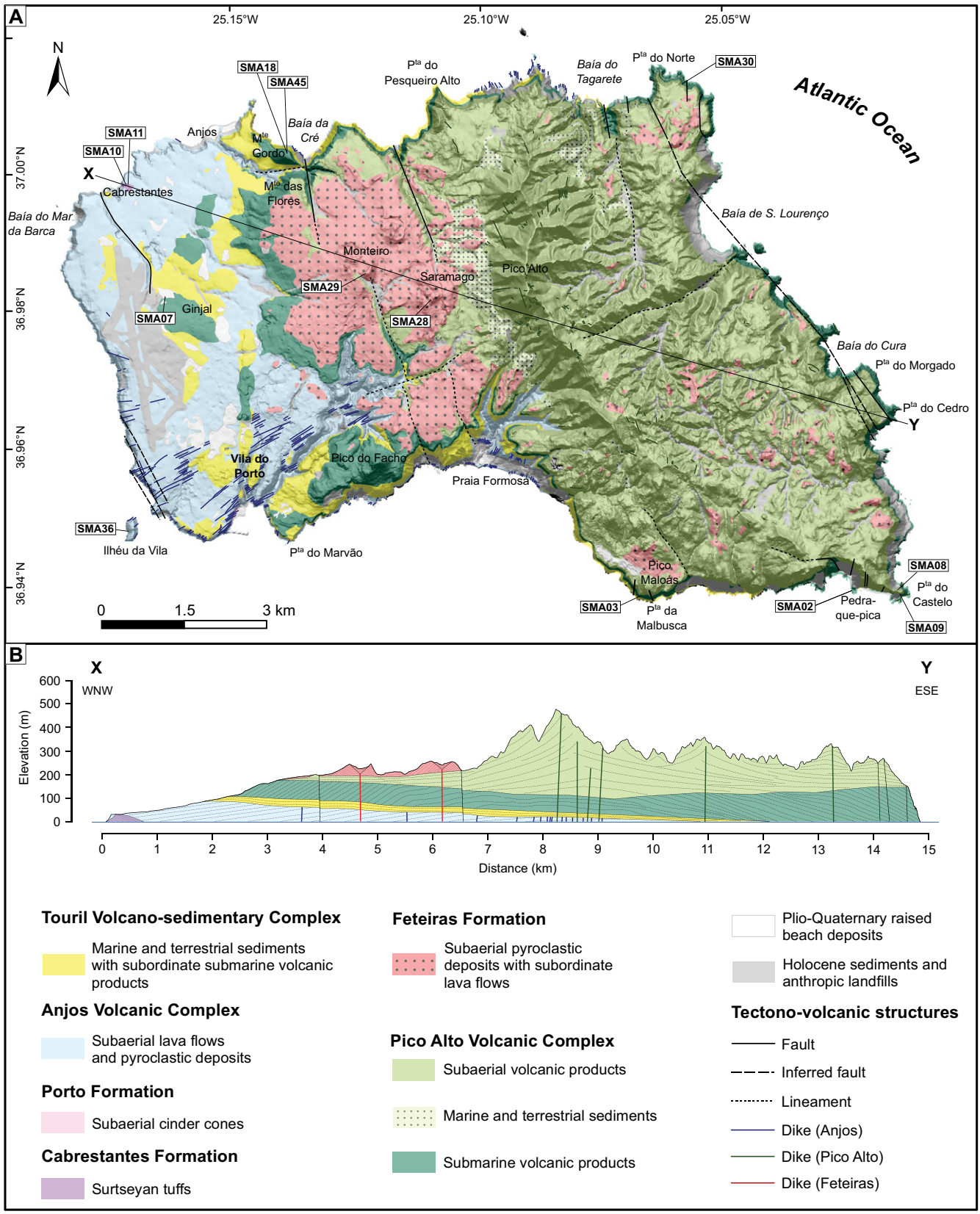

Figure 2. (A) Geological map of Santa Maria Island after Serralheiro et al. (1987), with (B) a WNW-ESE cross section, and key for both map and section (Porto Formation is not visible at this scale). Approximate sample locations are plotted in the map. "Pta" and "Mte" are abbreviations for "Ponta" and "Monte," respectively. Underlying digital elevation model was generated from a 1:5000 scale digital altimetric database.

edifice. Exposures along the coastal cliffs were surveyed during several boat trips to document the first- and second-order stratigraphic relations exposed around the full circumference of the island. Whenever necessary, the elevation of individual horizons (relative to present sea level) was measured using an Impulse 200LR laser distance meter produced by Laser Technologies, Inc.™, with a range up to 500 m. This equipment was also used to estimate the apparent vertical displacement of faults, by measuring the elevation difference between easily identifiable marker horizons that occur on adjacent fault blocks.

Uplift tracers used in this study corresponded to paleo–relative-sea-level markers, as defined by Ramalho et al. (2010a, 2010b, 2010c) and Ramalho (2011). Priority was given to markers representing the passage zone between subaerial and submarine lava flows within effusive lava deltas, since this feature marks very accurately the contemporaneous position of sea level (Jones and Nelson, 1970; Cas and Wright, 1987; Porębski and Gradziński, 1990; Ramalho et al., 2010a, 2010b, 2010c; Ramalho, 2011; Meireles et al., 2013). After carefully selecting the dating targets, samples were collected for later analysis in the laboratory.

Tracing of Pliocene–Quaternary Shorelines

The geomorphology of Santa Maria was analyzed in detail in order to map the position of each of the Pliocene–Quaternary marine terraces found on the island. We traced the outline of the inner edge of each terrace (i.e., the shore angle of each paleoshoreline) using stereoscopic aerial photo interpretation (color vertical imagery from September 2005, at an approximate scale of 1:18,000) and a 2-m-spatial-resolution digital elevation model (DEM) generated from a 1:5000 scale altimetric database. The shore angle of each paleoshoreline can be generally assumed to represent, within few meters of accuracy, the relative-sea-level position coeval with that shoreline (Rovere et al., 2016). These measurements were complemented by field observations and localized differential global positioning system (GPS) surveys, in order to determine the position and elevation of the inner edges with greater accuracy and resolution. To this purpose, we used a Trimble GPS equipped with Omnistar real-time differential corrections (HP service) that allowed us to reach vertical measurement accuracies of 8–10 cm. Trenches were also dug to confirm the presence of marine sediments at a selected terrace, and to recover dateable material. Our paleoshoreline reconstructions were then plotted in the same 2-m-spatial-resolution DEM.

$^{40}Ar/^{39}Ar$ Geochronology

The $^{40}Ar/^{39}Ar$ analyses were performed at the U.S. Geological Survey (USGS) in Denver, Colorado. Fresh rock fragments (~1 mm^3) free of obvious alteration and mineral grains of sanidine were prepared using crushing, picking, and heavy liquid techniques. The basalt samples were irradiated for 0.5 MWh, and the sanidine sample was irradiated for 0.17 MWh in the central thimble position of the USGS TRIGA reactor (Dalrymple et al., 1981), while also being rotated at 1 rpm. Following irradiation, the basalt fragments and sanidine samples and standards were loaded with tweezers into a stainless-steel sample holder and then placed into a laser chamber with an externally pumped ZnSe window. The volume of the mostly stainless-steel vacuum extraction line, including a cryogenic trap operated at –130 °C and two SAES™ GP50 getters (one at room temperature, one operated at 2.2 A), is estimated at ~450 cm^3. A combination of turbo molecular pumps and ion pumps maintained steady pressures within the extraction line of $<1.33 \times 10^{-7}$ Pa. Samples were incrementally heated in steps of 90 s, by controlled power output of a 50 W CO_2 laser equipped with a beam-homogenizing lens, resulting in uniform energy over the entire sample surface. During laser heating, any sample gas released was exposed to the cryogenic trap and was further purified for an additional 120 s by exposure to both the cryogenic trap and the SAES getters. The sample gas for all basalt samples was expanded into a Thermo Scientific ARGUSVI™ mass spectrometer, and argon isotopes were analyzed simultaneously using four Faraday detectors (^{40}Ar, ^{39}Ar, ^{38}Ar, ^{37}Ar) and one ion counter (^{36}Ar). Analytical data for the one sample of sanidine unknowns (SMA07) were analyzed by peak hopping on an electron multiplier in analog mode on a Mass Analyzer Products™ 215–50 mass spectrometer. Following data acquisition of 10 min, time zero intercepts were fit to the data (using parabolic and/or linear best fits) and corrected for backgrounds, detector intercalibrations, and nucleogenic interferences. The Masspec computer program written by A. Deino of the Berkeley Geochronology Center was used for data acquisition, age calculations, and plotting. All $^{40}Ar/^{39}Ar$ ages reported in Table 1 are referenced to an age of 28.201 ± 0.046 Ma for the Fish Canyon sanidine (Kuiper et al., 2008), the decay constants of Min et al. (2000), and an atmospheric $^{40}Ar/^{36}Ar$ ratio of 298.56 ± 0.31 (Lee et al., 2006). Laser fusion of >10 individual Fish Canyon Tuff sanidine crystals at each closely monitored position within the irradiation package resulted in neutron flux ratios reproducible to ≤0.25% (2σ). Isotopic production ratios were determined from irradiated CaF_2 and KCl salts, and for this study the following values were measured: $(^{36}Ar/^{37}Ar)_{Ca} = (2.45 \pm 0.05) \times 10^{-4}$; $(^{39}Ar/^{37}Ar)_{Ca} = (6.59 \pm 0.10) \times 10^{-4}$; and $(^{38}Ar/^{39}Ar)_{K} = (1.29 \pm 0.03) \times 10^{-2}$. Cadmium

TABLE 1. SUMMARY OF $^{40}Ar/^{39}Ar$ GEOCHRONOLOGY RESULTS OF PALEO–SEA-LEVEL MARKER INFORMATION USED IN THIS STUDY

Stratigraphic unit	Sample ref.	Location	Coordinates (WGS84)	Elevation of paleo–sea-level marker (m)	Tectonic correction	Age (Ma ± 2σ)
Cabrestantes	SMA10	Cabrestantes	36.99828°N, 25.17193°W	37	–	5.80 ± 0.3
Cabrestantes	SMA11	Cabrestantes	36.99835°N, 25.17199°W	37	–	6.01 ± 0.14
Anjos	SMA36	Ilhéu da Vila	36.94187°N, 25.17270°W	11	–	5.84 ± 0.09
Touril	SMA02	Pedra-que-pica	36.93011°N, 25.02569°W	8	12	4.78 ± 0.13
Pico Alto	SMA08	Ponta do Castelo	36.92981°N, 25.01639°W	91	12	3.98 ± 0.05
Pico Alto	SMA09	Ponta do Castelo	36.92947°N, 25.01673°W	55	12	4.13 ± 0.19
Pico Alto	SMA03	Ponta da Malbusca	36.93017°N, 25.06856°W	130	–	4.08 ± 0.07
Pico Alto	SMA30	Ponta do Norte	37.01257°N, 25.05641°W	110	50	3.52 ± 0.04
Pico Alto	SMA18	Monte Gordo	37.00349°N, 25.13888° W	190	–	3.63 ± 0.09
Pico Alto	SMA45	Monte Gordo	37.00344°N, 25.13876°W	190	–	3.71 ± 0.08
Feteiras	SMA28	Saramago	36.97879°N, 25.11020°W	215 and 130*	–	3.22 ± 0.13
Feteiras	SMA29	Monteiro	36.98254°N, 25.12535°W	215 and 130*	–	2.92 ± 0.08
Pliocene–Quaternary sediments	SMA07	Ginjal	36.97928°N, 25.16365°W	85	–	2.15 ± 0.03

Note: All reported ages are shown with 2σ levels of uncertainty. WGS84—World Geodetic System 1984.

*The cones of Feteiras lie over the 210–230 m marine terrace, but their subaerial products reach down to 130 m; these cones therefore provide a lower age bound for the 210–230 m paleoshoreline (here indicated with the medium elevation of 215 m) and an upper age bound for the 130 m paleoshoreline.

shielding during irradiation prevented any measurable $(^{40}Ar/^{39}Ar)_K$. The $^{40}Ar/^{39}Ar$ plateau ages (and uncertainties) are considered the best estimate of the age of the basalt samples and were calculated from samples if three or more consecutive heating steps released ≥50% of the total ^{39}Ar and also had statistically indistinguishable $^{40}Ar/^{39}Ar$ ages. If samples nearly met these criteria, a preferred weighted mean age was calculated; otherwise, the integrated age was used as the preferred age of the basalt. For samples dated by single-crystal laser $^{40}Ar/^{39}Ar$ fusion, a weighted mean was calculated from grains considered to represent a single age population and excluding any clear outliers.

Uplift Reconstructions

Uplift reconstructions were made using the method established by Ramalho et al. (2010a, 2010c) and Ramalho (2011). A comparison between relative sea-level positions and coeval eustatic sea level was established in order to infer vertical displacements and reconstruct uplift/subsidence trends. The Miller et al. (2005) eustatic curve was used as a reference, since it is one of the few curves spanning the ~6.5 m.y. time interval required for this study. Uncertainties in sea level, as well as the effects of glacio-isostatic adjustment in relative sea level, were not factored into this first-order approximation. This is because our reconstructions span several million years, and the majority of the relative sea-level markers used in this study correspond to volcanic tracers that could have been formed at any given time within a glacio-eustatic cycle. Additionally, since some of the chosen uplift tracers were vertically offset by local faults, a "tectonic correction" was applied to those tracers located on adjacent downthrown blocks; this was done simply by adding the apparent vertical fault displacement into their elevation, in order to minimize local tectonic effects on relative sea-level differences. This "tectonic correction," however, was only applied to uplift tracers located within a short distance to each other, and not to tracers located in different parts of the island, because there is less control of vertical tectonics at that scale. Finally, all elevation values are given in meters above or below (when preceded by "–") present mean sea level (local datum).

RESULTS

Uplift Tracers

Cabrestantes and Porto Formations

Outcrops of the Cabrestantes Formation at Ribeira dos Cabrestantes correspond to the eroded remnant of a Surtseyan cone, implying an eruption from a vent located in shallow water. It is not known for certain whether this outcrop corresponds to the submarine base of the cone or its emergent (subaerial) summit; i.e., it is not possible to assert with precision where relative sea level was at the time of its extrusion. However, the tuffs are generally even- and planar-bedded, without any cross-stratification, bomb sags, or other signs of surge deposition and subaerial ballistic impacts. Consequently, we interpret this outcrop as water-settled and therefore suggest that relative sea level was above the eroded top of the present outcrop. We therefore assign an elevation of 37 m as a first-order approximation for coeval relative sea level. In order to constrain the age of this cone, two samples (SMA10 and SMA11) corresponding to two different volcanic bombs were collected at this site.

The cones of Porto Formation (sensu Serralheiro et al., 1987) correspond to Strombolian vents and therefore were erupted subaerially. Their presence, together with the outcrop at Cabrestantes, attests to the transition from submarine to subaerial volcanism during island emergence. The fact that these outcrops occur at the same elevations as the succession at Cabrestantes shows that there was probably a small relative lowering of sea level in between the extrusion of these units, confirmed by the transition between Surtseyan and Strombolian volcanism.

Anjos Volcanic Complex

As reported by previous authors (e.g., Serralheiro et al., 1987; Serralheiro, 2003; Ávila et al., 2012; Sibrant et al., 2015a), the exposed Anjos volcanic edifice is overwhelmingly subaerial in nature. At Ilhéu da Vila (Fig. 2A) and Baía do Mar da Barca, however, it is possible to find submarine morphologies intercalated within the subaerial sequence. These outcrops mark the position of sea level during one or two distinct moments during the extrusion of the shield volcano and therefore constitute ideal targets to track uplift/subsidence. The sequence is particularly clear at Ilhéu da Vila, where a former coastline is preserved at ~11 m in elevation (Fig. 3A). Here, a shore platform carved on subaerial flows is overlain by a boulder beach, which is in turn covered by a thick subaerial lava flow, the base of which entered the water, generating pillowed structures. This passage zone therefore demarks the position of sea level during the extrusion of the lava flow, and so it was sampled for geochronology (sample SMA36). The sequence at Baía do Mar da Barca marks relative sea level at approximately the same elevation. As for the rest of Anjos volcanic complex, relative sea level was well below present sea level, perhaps suggesting that these submarine morphologies were formed during short-lived glacio-eustatic highstands when relative sea level was particularly high.

Touril Volcano-Sedimentary Complex

The Touril volcano-sedimentary complex (Figs. 3B–3D, 3F) corresponds to a dominantly clastic sedimentary sequence (conglomerates, sandstones, calcarenites, and rare limestones) intercalated by hydromagmatic tuffs and submarine effusive products (particularly on the southern side of the island). This sequence varies laterally and vertically in characteristics but in general grades from coarser terrigenous conglomerates in the lower part of the succession toward finer fossiliferous marine conglomerates, sandstones, calcarenites, and limestones near the top of the succession (Serralheiro, 2003; Ávila et al., 2012). These deposits therefore grade upward from highly energetic terrigenous sediments to an increasingly open-marine character toward the top, a situation also reflected in their fossil content (e.g., Serralheiro, 2003; Janssen et al., 2008; Ávila et al., 2012, 2017). This transition suggests that relative sea level gradually rose throughout the time period spanned by this unit. We cannot quantify the extent of this sea-level rise in detail, but it must have exceeded 70–80 m, the maximum thickness of the sequence. The maximum elevation at which the Touril complex presently occurs is ~120 m. A single sample was collected in this unit (SMA02), corresponding to the pillow lavas that form the base of the sequence (at 8 m in elevation) of Pedra-que-pica/Ponta do Castelo, described later in this text.

Pico Alto Volcanic Complex

The Pico Alto volcanic complex makes up the bulk of the eastern part of Santa Maria's volcanic edifice, and it provides abundant relative sea-level markers that are superbly exposed along the island's southern, eastern, and northern coastal cliffs (Figs. 3B–3H). This unit is largely composed of effusive sequences with submarine characteristics at the base (with occasional intercalated marine sediments) and subaerial characteristics at higher elevations. The passage zone between the submarine and subaerial portions of the complex is located between ~50 and ~200 m in elevation, and it is generally found at increasingly higher elevations toward the eastern and western fringes of the volcanic edifice (see Fig. 2B). The internal structure of Pico Alto volcanic complex shows that, in the southern, northern, and western parts of the island, the underlying sedimentary sequence of Touril has been overlain by thick lava-fed delta sequences, either exhibiting the typical

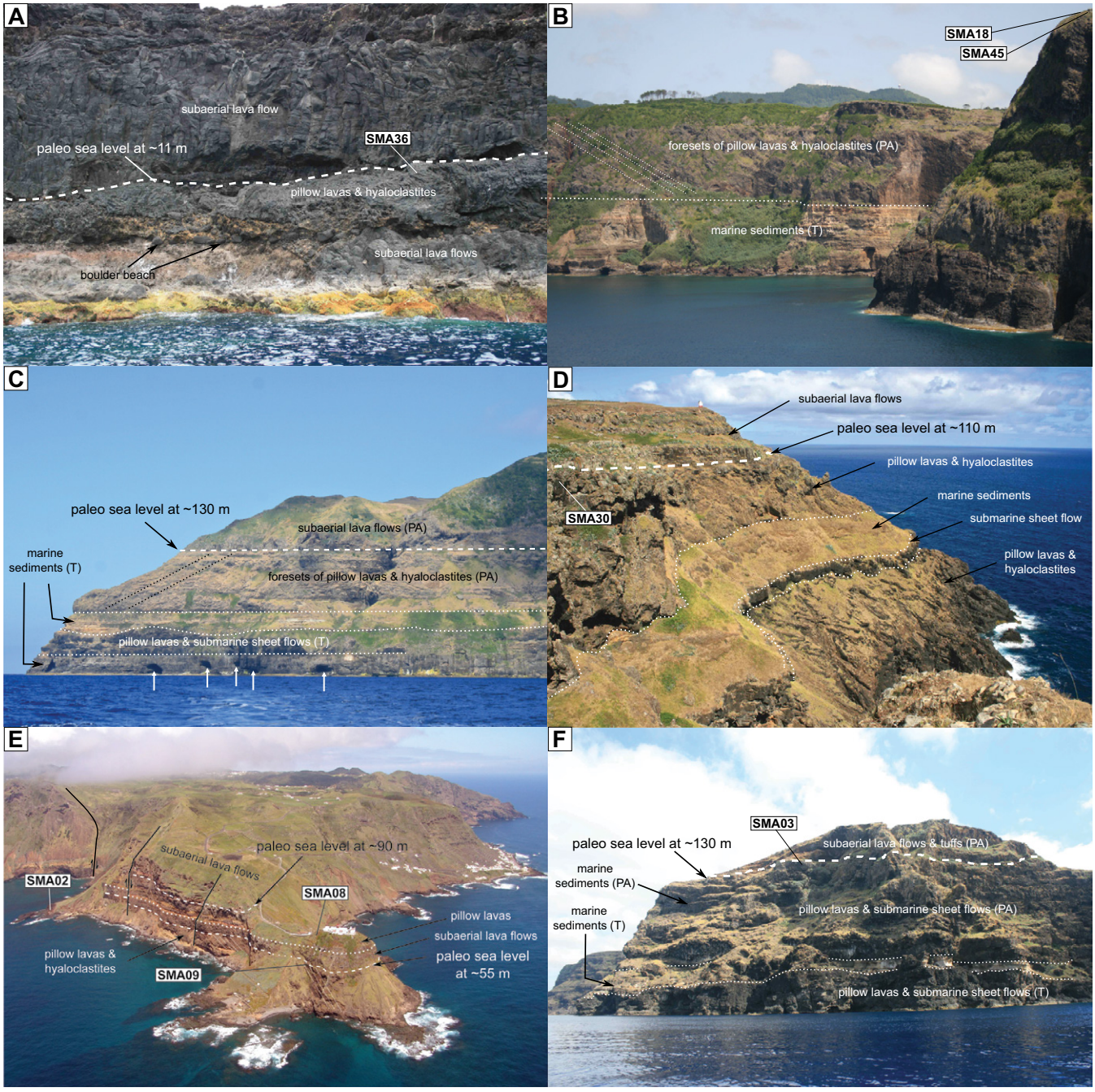

Figure 3 (*on this and following page*). Photographs of representative paleo–sea-level markers used in this study. (A) Section at Ilhéu da Vila (looking NE), showing a paleo–sea-level at ~11 m, within the Anjos volcanic succession. Here, a subaerial lava flow formed pillow structures and hyaloclastites as it entered the sea, over a beach developed on subaerial lava flows. (B) Section exposed at Baía da Cré (looking SSE). The marine sedimentary sequence of the Touril (T) complex is overlapped by a west-prograding lava-fed delta belonging to the Pico Alto volcanic complex (PA); the passage zone is exposed at ~200 m (west of Cré fault) and ~130 m (east of Cré fault) in elevation. (C) Section at Ponta do Pesqueiro Alto (looking E), consisting of marine sediments and submarine effusive sequences of the Touril complex (T), overlapped by a northward-prograding lava-fed delta of the Pico Alto volcanic complex (PA); passage zone is located at ~130 m in elevation. White vertical arrows show marine oxygen isotope stage 5e (MIS5e) wave-cut notches. (D) Section at Ponta do Norte (looking WNW), showing overlapping lava-fed deltas and intercalated marine sediments of Pico Alto volcanic complex; passage zone is exposed at ~110 m in elevation, where sample SMA30 was collected. (E) Section at Pedra-que-pica/Ponta do Castelo (looking NW). Here, two conformably overlapping lava-fed deltas can be seen, marking two paleo–sea levels at ~90 m and ~55 m, where samples SMA08 and SMA09 were collected, respectively; sample SMA02 was also collected from the basal pillow lavas of the Touril complex. (F) Section at Ponta da Malbusca (looking N), showing the vertical stacking of submarine effusive sequences and marine sediments belonging to the Touril (T) and Pico Alto volcanic complex (PA). The passage zone occurs at ~130 m in elevation, where sample SMA03 was collected.

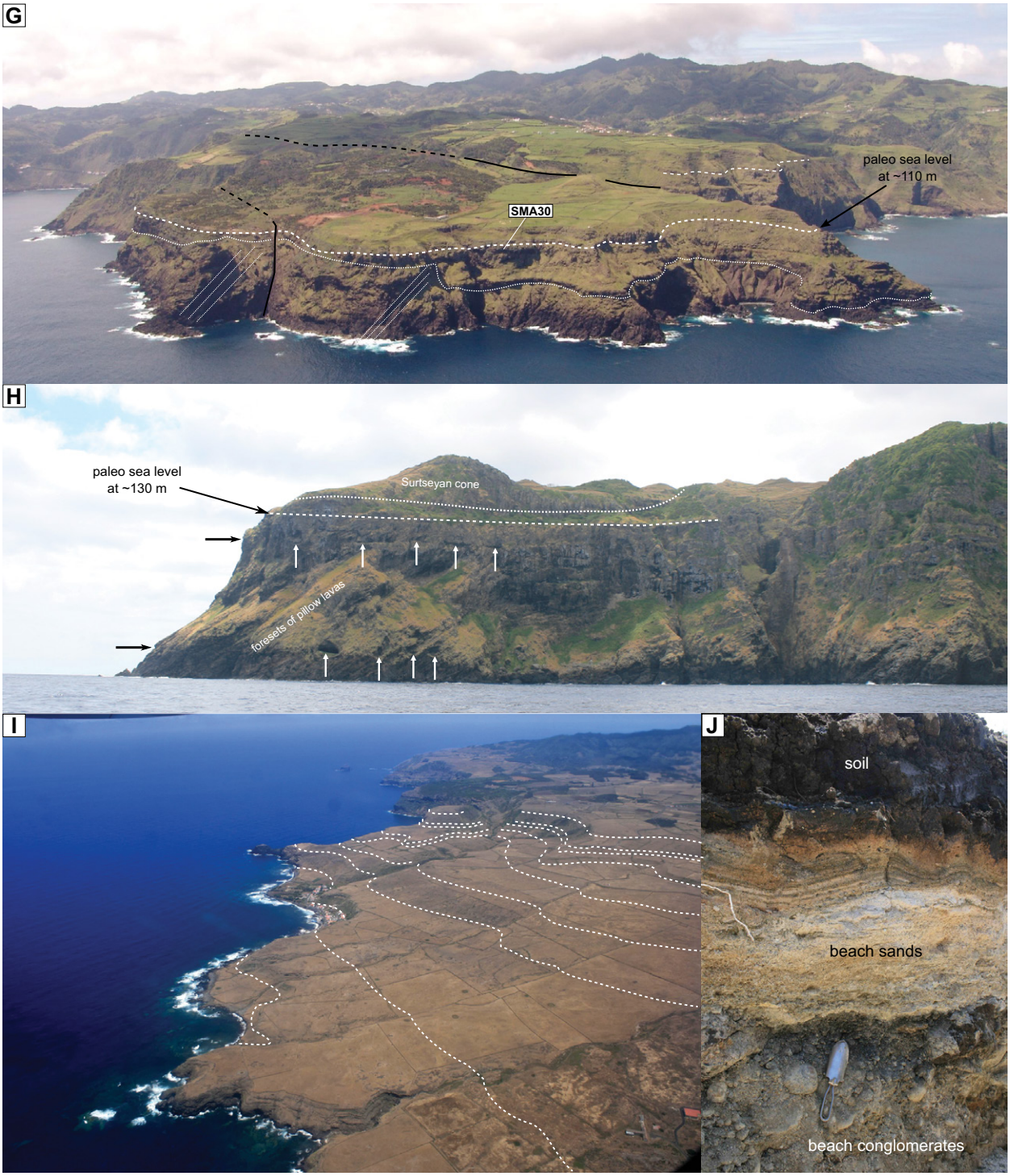

Figure 3 (*continued*). (G) Sequence at Ponta do Norte (looking S). Here, a younger lava-fed delta of Pico Alto volcanic complex unconformably overlaps an older lava delta of the same unit, prograding to the ENE. The passage zone on the younger lava-fed delta occurs at ~110 m in elevation, but the same passage zone can be seen at ~160 m in elevation across the Ponta do Norte fault, which has ~50 m of apparent vertical displacement. (H) Section at Ponta do Morgado/Baía do Cura (looking SSE) exhibiting a textbook example of a Gilbert-type lava-fed delta, prograding to the east, with the passage zone at ~130 m in elevation. The vertical continuity of the eastward-dipping foresets of pillow lavas and hyaloclastites from ~130 m to present sea level shows that volcanic progradation extended beyond the coeval insular shelf edge. Note also the presence of wave-cut notches at 18–20 m and 105–110 m in elevation (indicated by the black and white arrows). (I) Staircase of marine terraces at the northeastern part of the island (looking ENE); dashed lines mark the position of former shorelines. (J) Pleistocene beach composed of beach conglomerates (including rounded stranded pumice) and fossiliferous calcarenites exposed in a trench near Ginjal. The presence of this former beach at 85–90 m attests to the position of a paleoshoreline at these elevations.

prograding "pillow and hyaloclastite" Gilbert-type structure, or, more rarely, the geometry of aggradational lava-fed deltas composed of submarine sheet flows (for details on these types of lava-fed deltas, see Ramalho et al., 2013). The contact between the Touril and the Pico Alto sequences in these areas is relatively flat, dipping gently toward the eastern part of the island, where it disappears below sea level. This contact is generally conformable, except on the western part of the island (e.g., at the base of Pico do Facho), where a smooth unconformity is present, attesting to some degree of consolidation by the sediments and slight erosion prior to the deposition of the volcanic sequences above. In the eastern part of the island, the structure of Pico Alto volcanic edifice almost exclusively corresponds to extensive "pillow and hyaloclastite" Gilbert-type lava-fed deltas, consistently prograding to the eastern quadrant. Across the area, the steeply dipping, "foreset units" of these lava-fed deltas extend continuously from their passage zone at elevations up to ~130 m down to present sea level (e.g., at Ponta do Morgado; Fig. 3H). In places, however, younger lava-fed deltas lie conformably or unconformably above the initial lava delta sequence, providing additional information on relative sea-level change. Since the passage zone in all these lava deltas very accurately marks where relative sea level was at a given point in the history of the Pico Alto volcanic edifice, several key sections were selected and studied in detail in order to get a representative overview of relative sea-level change during this phase of the construction of the island.

Monte Gordo/Monte das Flores. All across the western part of the Pico Alto volcanic edifice, the structure corresponds to westward-prograding Gilbert-type lava-fed deltas, either lying directly over the Touril marine sediments, or above a thin set of laterally very extensive submarine sheet flows that cap the Touril sequence. The passage zone in these lava deltas is generally at 180–200 m, corresponding to the highest elevation at which this sea-level marker occurs within the Pico Alto edifice. The sequence is particularly well exposed around Monte Gordo and Monte das Flores in the northern part of the island (see Figs. 2A and 3B), where the passage zone can be observed at ~200 m; samples SMA18 and SMA45 were collected in the submarine lava flows immediately below this passage zone, in Monte Gordo, and constitute the highest, directly dateable paleo–sea-level marker in Santa Maria.

Ponta do Pesqueiro Alto. Immediately to the east of Monte Gordo, along the northern coast, the same passage zone is located at ~130 m in elevation, due to the 60–70 m vertical displacement on the Cré fault; this passage zone, however, can be traced several kilometers to the east, to Ponta do Pesqueiro Alto (Fig. 3C), where it still occurs at ~130 m. Here, a tabular sequence of marine conglomerates, submarine flows, and marine sediments of the Touril complex is overlain by a northward-prograding Pico Alto lava delta, with a very clear passage zone.

Ponta do Norte. At Ponta do Norte, on the northern coast (Figs. 3D and 3G), two lava delta sequences are stacked unconformably with marine sediments intercalated in between them. Pillow lava foresets (dipping to ENE) of the older lava delta reach up to ~100 m in elevation (being truncated at the top), and the younger lava delta exhibits its passage zone at 110 m, where sample SMA30 was collected. This entire sequence, however, is downthrown ~50 m relative to the island's mainland, along a NNW-striking vertical fault (see Fig. 2).

Ponta do Morgado/Ponta do Cedro. The coastline that extends from the southern end of Baía de São Lourenço to Ponta do Cedro offers one of the best exposures in the island. This entire stretch of coast corresponds to a long-lived Gilbert-type lava-fed delta, prograding to the eastern quadrant, the passage zone of which ranges from ~80 m in the inner part of the delta (e.g., within Baía do Cura) to ~130 m in the outer part of the delta (e.g., Ponta do Morgado; Fig. 3H).

Ponta do Castelo/Pedra-que-pica. At Ponta do Castelo (Fig. 3E) on the southeastern tip of the island, two conformably overlapping lava delta sequences constitute distinct relative sea-level markers at 55 m and 90 m, where samples SMA09 and SMA08 were collected, respectively (for more details on these sequences, refer to Meireles et al., 2013; Ávila et al., 2015a, 2015d). Sample SMA02 was also collected from the pillow lavas that form the base of the sequence (at 8 m in elevation) at Pedra-que-pica, which correspond to the top of the Touril complex. The sequences at Ponta do Castelo and Pedra-que-pica are, however, displaced by a set of down-to-the-east faults with a total apparent vertical displacement of ~12 m.

Ponta da Malbusca. At Ponta da Malbusca (Fig. 3F), in the southern coast, the sequence consists of a subhorizontal stack of pillow lavas and marine sediments belonging to the Touril complex, overlain by submarine sheet flows and marine sediments of the Pico Alto complex, which transition to subaerial flows and tuffs at ~130 m. Here, the overall Pico Alto sequence corresponds to an aggradational lava-fed delta, generated by the vertical stacking of thick and laterally extensive submarine sheet flows and subordinate marine sediments, accompanied by a relative sea-level rise of at least 60 m (Rebelo et al., 2016). Sample SMA03 was collected in the highest submarine lava flow in the sequence, in order to date this relative sea-level tracer.

Feteiras Formation

The Feteiras Formation corresponds to a set of monogenetic hydromagmatic and magmatic cones (and associated pyroclastic deposits and lava flows), mostly concentrated on the central part of the island, which features a broad plateau at the foot of the Pico Alto range. This plateau has been interpreted as a Pliocene marine terrace, presently located at 200–230 m in elevation, over which surface these cones were emplaced (Serralheiro et al., 1987; Serralheiro, 2003; Ávila et al., 2012). To obtain an upper age bound on this surface, samples SMA28 and SMA29 were collected at the cones of Monteiro and Saramago, respectively (Fig. 2A). Since the products of this volcanic stage have been mapped by Serralheiro et al. (1987) down to ~130 m, the age of these cones (at least the youngest) could also be used as a first-order approximation to the minimum age of any marine terraces above that elevation.

Pliocene–Quaternary Shoreline Reconstructions

Our geomorphological reconstructions revealed the presence of 10 recognizable uplifted paleoshorelines at ~7–11 m, 45–50 m, 55–60 m, 65–70 m, 85–90 m, 105–110 m, 120–125 m, 140–145 m, 155–165 m, and 210–230 m in elevation (see Figs. 3I and 4A–4C). The succession of marine terraces and the resulting staircase morphology are particularly evident on the NW section of the island, from Anjos toward Monte Gordo and Monte das Flores, and also in the SW, from Ponta do Marvão toward Pico do Facho (see Fig. 4A). The uncertainty in our reconstructions increases with elevation due to increasingly more severe topographical decay and later volcanic cover. The outline of the higher 210–230 m paleoshoreline is particularly poorly constrained, and it is crudely estimated by a marked slope break (and morphology contrast) at the foot of the Pico Alto range. In a similar fashion, due to anthropogenic landscape alterations (e.g., terrain leveling and landfill), the area surrounding Santa Maria's airport is equally problematic. In contrast, the position and outline of the lower marine isotope stage (MIS) 5e shoreline (7–11 m in Fig. 4A) are well constrained and have been the subject of previous studies in the Azores (e.g., Ávila et al., 2009, 2015c, 2015d; Ramalho et al., 2013; Meireles et al., 2013). The range in elevation of MIS 5e notches and terraces in Santa Maria is generally in accordance with studies

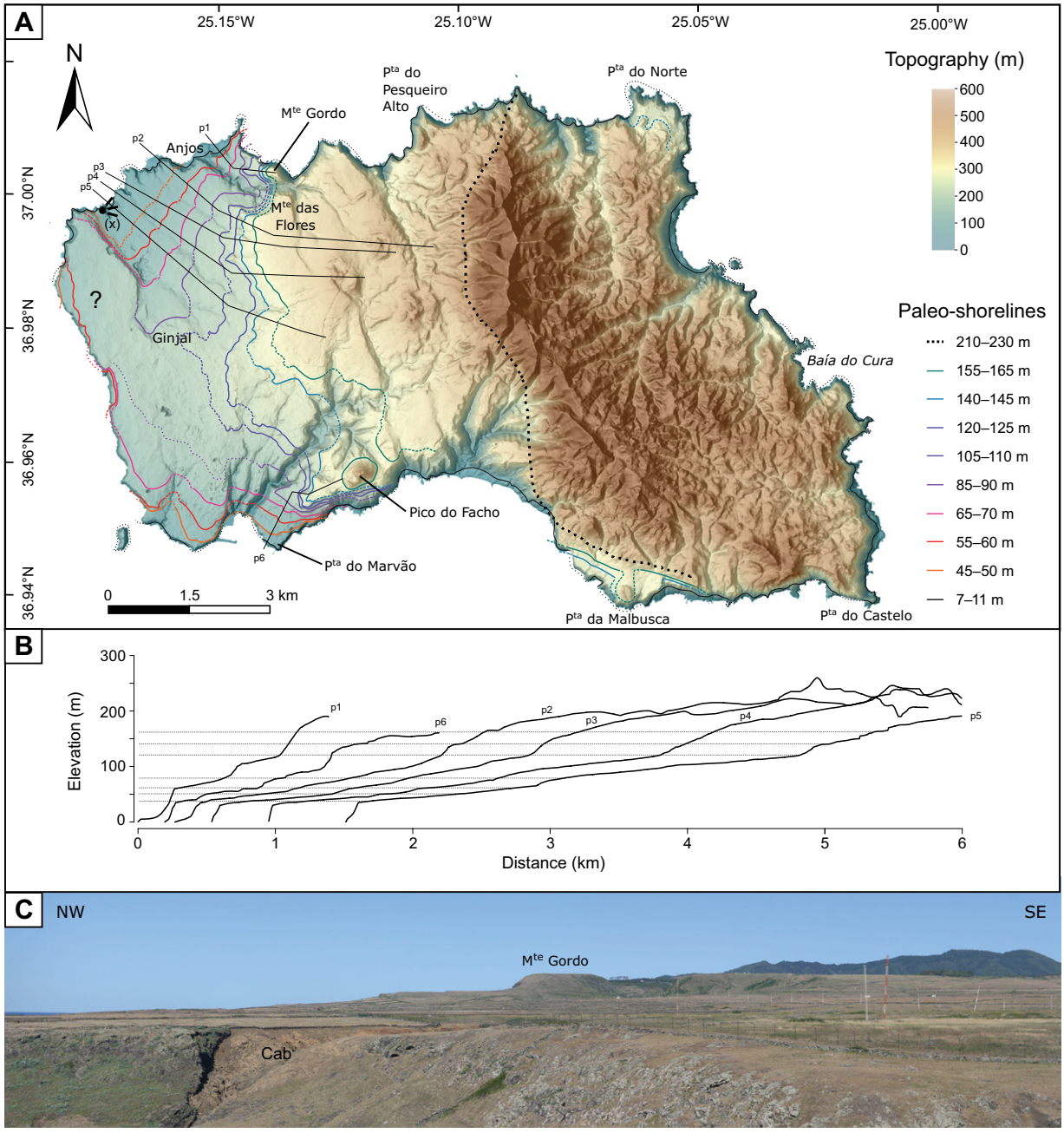

Figure 4. (A) Pliocene–Quaternary paleoshoreline reconstructions based on uplifted marine terrace morphology. Lines represent the inner edge of each terrace, i.e., the position of the former shore angle (solid line—visible/high confidence; dashed line—interpreted/medium confidence; dotted—interpreted/low confidence). Digital elevation model was generated from a 1:5000 scale digital altimetric database. "P^{ta}" and "M^{te}" are abbreviations for "Ponta" and "Monte," respectively. (B) Cross-shore profiles (p1–p6) taken along solid black lines represented in A; marine terraces are clearly visible in these profiles (horizontal dotted lines). (C) Photo of marine terrace staircase morphology taken from point x in A, looking to the ENE. Note also the Cabrestantes Formation (Cab) in the foreground.

of the peak MIS 5e highstand elsewhere around the world (e.g., Hearty et al., 2007; Kopp et al. 2009; Dutton and Lambeck, 2012; O'Leary et al., 2013), despite the fact that our observations were not corrected for isostatic adjustment (Creveling et al., 2015).

The lack of well-developed marine terraces (other than MIS5e) on the southeastern, eastern, and northeastern sides of the island is noteworthy. However, in several places along these coastlines, wave-cut notches are clearly visible at several elevations across the plunging cliffs, attesting to the relative position of sea level at the aforementioned elevations. Apart from the ubiquitous MIS5e notches and terraces, which can be observed at 7–11 m in elevation at numerous locations around the island, rarer (and presumably older) notches have also been re-

corded at 18–20 m (e.g., at Ponta da Malbusca and Baía do Cura) or even at 105–110 m (at Ponta do Morgado/Baía do Cura; see Fig. 3H).

Field reconnaissance revealed the presence of loose remains of Pleistocene fossiliferous calcarenites in a small area to the NW of Ginjal, next to the marked inner edge of the 85–90 m paleoshoreline, as originally reported by Serralheiro et al. (1987). Trenches at this locality revealed a Pleistocene beach 1 m below the surface. The beach deposits (Fig. 3J) exhibit a basal conglomerate covered by microconglomerates of rounded stranded pumice (transported to Santa Maria as flotsam from another island) and bioclast-rich sand, featuring typical very shallow foreshore fossil assemblages (e.g., vermetids and limpet shells of the extant *Patella aspera* Röding, 1798, regarded as solid biological relative sea-level indicators; Rovere et al., 2015). This sequence therefore marks very accurately the relative position of sea level, and, since the age of the stranded pumice can be considered penecontemporaneous with coastal deposition (as sea wrack in a high tidal area), it provides rare and fortuitous dateable material with which to track Quaternary uplift. A pumice sample (SMA07) was thus collected for $^{40}Ar/^{39}Ar$ geochronology.

$^{40}Ar/^{39}Ar$ Geochronology

Our $^{40}Ar/^{39}Ar$ geochronology results for Santa Maria's volcanic relative sea-level tracers range from 6.01 ± 0.14 Ma to 2.92 ± 0.08 Ma (Fig. 5; Table 1; age uncertainties 2σ throughout)[1] and are in general agreement with the ages reported by Féraud et al. (1980), Féraud et al. (1981), Storetvedt et al. (1989), and Sibrant et al. (2015a). The Surtseyan deposits of the Cabrestantes Formation yielded ages of 6.01 ± 0.14 Ma and 5.8 ± 0.3 Ma, results that overlap within their uncertainty envelope; given the larger uncertainty in the latter value, we assume the former to be a stronger age constraint for this sea-level tracer. These ages confirm the significance of this spatially restricted outcrop as the oldest unit in the island. The $^{40}Ar/^{39}Ar$ age of 5.84 ± 0.09 Ma for the paleocoastline within the subaerial Anjos shield volcano, at Ilhéu da Vila, is in reasonable agreement with the 5.70 ± 0.08 Ma age reported by Sibrant et al. (2015a) for the subaerial flows just opposite the channel on mainland Santa Maria. The three relative sea-level markers from the Pedra-que-pica/Ponta do Castelo cross section yielded, respectively, from the base to the top, 4.78 ± 0.13 Ma, 4.13 ± 0.19 Ma, and 3.98 ± 0.05 Ma. These values provide a consistent geochronology for the formation of this transgressive sequence. The youngest age also agrees with the 3.96 ± 0.06 Ma age reported by Sibrant et al. (2015a) further west of Ponta do Castelo. The sea-level marker at Ponta da Malbusca yielded 4.08 ± 0.07 Ma, which is also in good agreement with the 4.02 ± 0.06 Ma reported by Sibrant et al. (2015a) for the underlying upper submarine part of the sequence. These ages document rapid deposition of this volcano-sedimentary sequence during a transgressive period between 4.32 and 4.0 Ma, consistent with field relationships. The two samples collected at the lava delta sequence of Monte Gordo yielded ages of 3.71 ± 0.08 and 3.63 ± 0.09 Ma, providing a solid age estimate for this sea-level tracer. Farther east, the lava delta sequence at Ponta do Norte yielded 3.52 ± 0.04 Ma. Since this sequence unconformably rests on a former insular shelf carved on older similar structures belonging to an earlier stage of Pico Alto volcanic complex (Fig. 3G), it provides an age constraint on volcanic progradation late in the history of Santa Maria's eruptive life. The posterosional cones of Saramago and Monteiro yielded, respectively, 2.92 ± 0.08 Ma and 3.22 ± 0.13 Ma; the latter result, however, contrasts with the age of 3.52 ± 0.05 Ma reported by Sibrant et al. (2015a) for the same structure.

Single sanidine grains extracted from the pumice at Gingal (sample SMA07) yielded an age probability plot consistent with an $^{40}Ar/^{39}Ar$ age of 2.15 ± 0.03 Ma. We therefore consider an age of 2.1–2.2 Ma for the eruption of this pumice and consequently the same approximate age for its stranding along the coeval coastline at Santa Maria.

Uplift Reconstructions

Our uplift/subsidence reconstructions are presented in Figure 6, showing the position of sea level for each of the dated tracers relative to global mean glacio-eustatic sea level. Starting at present, the relative elevation of the dated sea-level tracers increases with increasing age until 3.5–3.7 Ma and then declines from there to ca. 5.8 Ma. These trends indicate that Santa Maria Island experienced ~100 m/m.y. of subsidence from ca. 5.8 Ma to 3.5–3.7 Ma, and then slower uplift (~60 m/m.y.) from then to the present. The minimum estimated uplift experienced by Santa Maria is solidly bound by the ca. 3.7 Ma passage zone at the Monte das Flores lava-fed delta at ~200 m in elevation. A weaker bound is provided by the inferred marine terrace at 210–230 m in elevation, which formed between 3.7 Ma (age of the underlying volcanic sequence) and 3.2 Ma (age of the oldest Feteiras cone). This minimum uplift is estimated to be about 180 m, if the elevation difference between the passage zone at Monte das Flores and their contemporaneous sea-level highstands (see Fig. 6) is used; if the long-term (averaged) sea-level curve is instead used as a reference, it corresponds to 205 m. Conversely, the minimum subsidence recorded during the earlier part of the island's history corresponds to ~200 m. Considering that the paleocoastline at Ilhéu da Vila dates to 5.84 Ma and is presently located at 11 m, the subtraction of 180 m of posterior uplift would bring this lower paleomarker to an elevation of –169 m, which represents a minimum negative vertical displacement of over 110 m below contemporaneous sea-level minima. If, on the other hand, one considers that this paleocoastline was instead formed during a highstand (more likely), the inferred subsidence is in excess of 190–200 m. As for the vertical movements that existed in between the Cabrestantes and the Anjos sea-level markers, it becomes almost impossible to constrain these with precision, because the elevation difference between the existing sea-level markers is small enough to fall within the coeval eustatic amplitude, and the age resolution is not precise enough to assert their exact position within the eustatic curve. Finally, it is worth mentioning that the tectonic corrections applied to some of the existing paleo–sea-level markers have little effect on the overall vertical movement reconstructions, attesting to the robustness of our analysis.

DISCUSSION

Uplift Reconstructions

The uplift reconstructions presented here, albeit with some uncertainty, clearly demonstrate that Santa Maria experienced a complex history of vertical motion, with subsidence followed by uplift. Despite the relative lack of dateable sea-level tracers spanning the last 3.5 m.y., which precludes any more precise uplift rate calculations, the inferred uplift trend is also clearly evidenced by the staircase of marine terraces present on the western side of the island (and the notches on the eastern side), and by the remains of a Pleistocene beach in one of those terraces, at 85–90 m in elevation. It is not possible, however, to discern episodic from continuous uplift solely on the existing data set. The older subsidence trend is more tightly constrained, on account of a richer record provided by the numerous passage zones of Pico Alto and Anjos lava deltas. This subsidence trend is equally demonstrated by the thick transgressive sequence of

[1]GSA Data Repository item 2016300, spreadsheet containing age calculation information and raw data for CO_2-laser incremental heating $^{40}Ar/^{39}Ar$ spectra of selected samples as presented in Figure 5, is available at http://www.geosociety.org/pubs/ft2016.htm or by request to editing@geosociety.org.

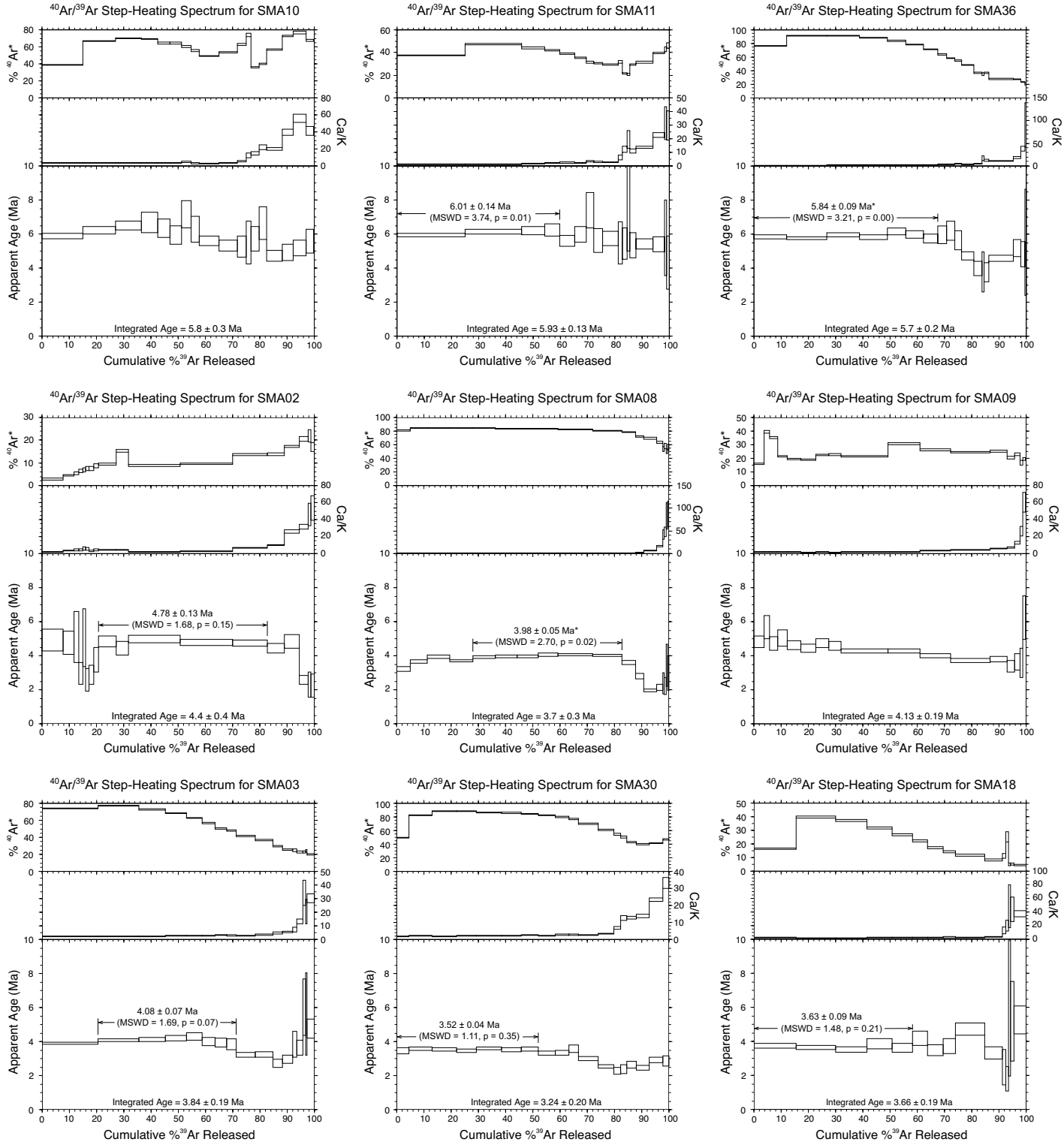

Figure 5 (*on this and following page*). Isotope correlation and age spectra (for comparison) for Santa Maria lavas. All reported ages (results) and the heights of boxes for individual heating steps (data) are shown with 2σ levels of uncertainty (except SMA07, which features data in 1σ, age results in 2σ). MSWD—mean square of weighted deviates.

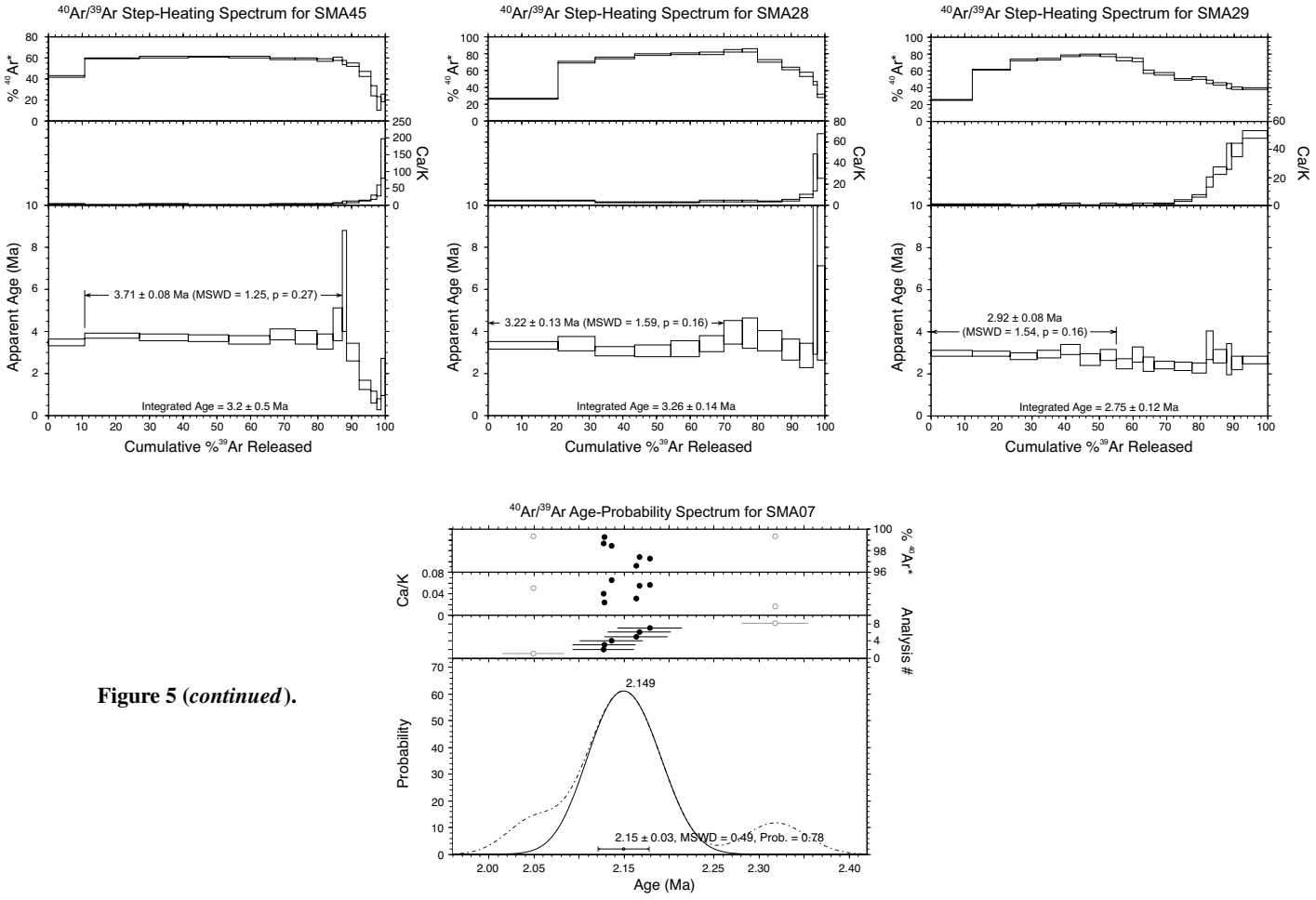

Figure 5 (*continued*).

the Touril complex, where the facies variation gradually increases in its more open-marine character toward the top.

Implications for Island Evolution

The $^{40}Ar/^{39}Ar$ geochronology results reported here provide a more solid constraint on the timing of first emergence above sea level by the island edifice and refine the existing time constraints on the several volcanic stages that took place to shape this edifice. More importantly, these results allow us to formulate a much clearer picture on the vertical movements affecting the island edifice throughout its evolutionary history, and how those movements may have affected that evolution.

Our work shows that Santa Maria Island first emerged by Surtseyan activity around 6 Ma (Fig. 7), as attested by the age of the Cabrestantes Formation. This foundational stage in the island evolutionary history was followed by a transition to the subaerial environment, initially through additional monogenetic volcanism (as attested by the Strombolian cone structures of the Porto Formation) and then through subaerial shield volcanism. The consolidation of the island edifice was thus probably sustained by an increase in magma production rates, which led to the formation of a shield volcano (corresponding to the Anjos volcanic complex) ca. 5.8–5.3 Ma. This shield volcano may have extended much further to the north and east, as both the volcanic structure and the northward extent of the present-day insular shelf both suggest. While the north side of the existing edifice was probably truncated by marine erosion, the retreat of the east side has been interpreted by Sibrant et al. (2015a) as the result of a flank collapse. Around 5.3 Ma, the edifice entered a period of pronounced subsidence that lasted until ca. 3.5 Ma; it is, however, expected that subsidence started much earlier in Santa Maria's geological history, with the loading of the submarine volcanic edifice. The total magnitude of subsidence recorded by the exposed sea-level tracers (~200 m, Fig. 6) is, nevertheless, 4–5 times what would be expected from thermal subsidence (~40 m; as inferred from the GDH1 model by Stein and Stein, 1992), and consequently may have been driven by surface loading imposed by vigorous volcanic activity. Subsidence rates determined by this study are an order of magnitude lower than those measured by recent GPS studies for other Azorean Islands (e.g., Trota, 2008; Catalão et al., 2011; Miranda et al., 2012; Marques et al., 2013) but are of the same order of magnitude as long-term determination of subsidence in the Azores by morphological proxies such as the shelf break depth (Quartau et al., 2014, 2015, 2016).

Following the construction of the Anjos shield volcano, the edifice entered a period of waning volcanism and erosion, which, aided by subsidence, resulted in the complete or almost-complete truncation of the existing island edifice to form a guyot (Fig. 7). This is well attested by the very flat unconformity between the Anjos and the Touril sequences, which can be followed semicontinuously from Praia Formosa to Baía do Tagarete, across the western side of the island. This period is recorded by the Touril volcano-sedimentary complex, which grades upward from high-energy terrigenous

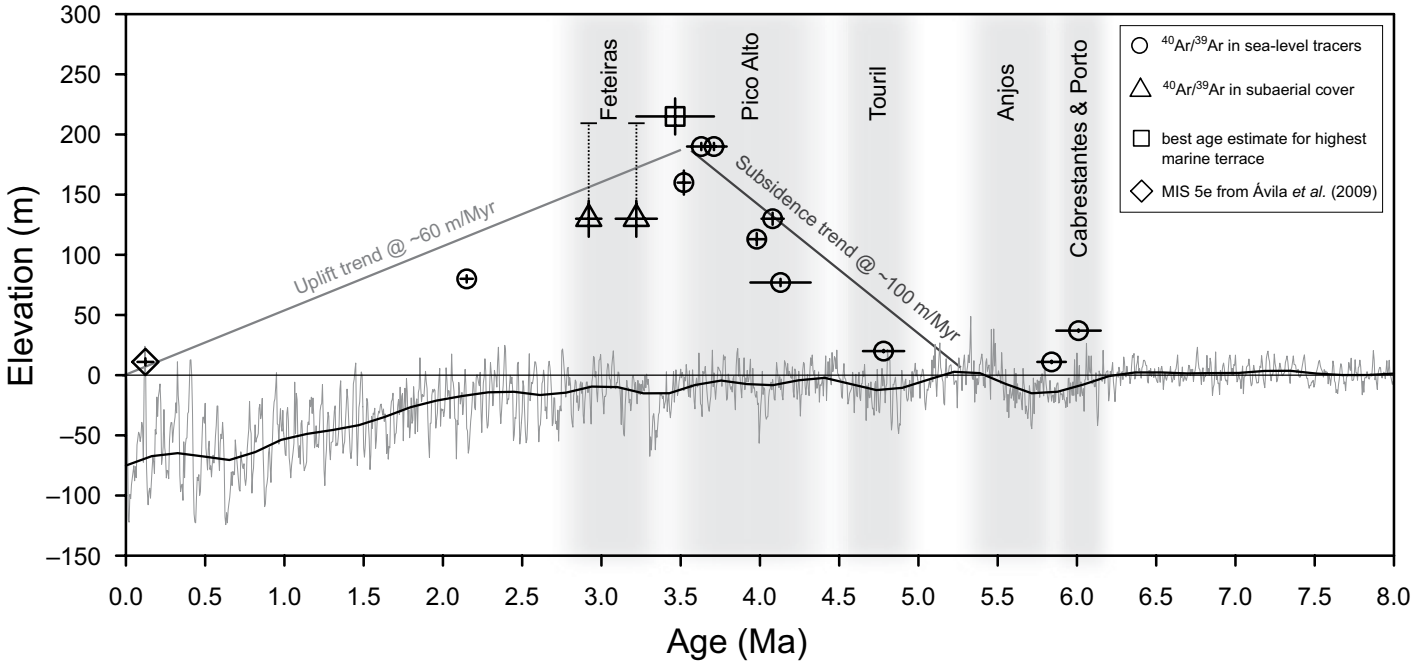

Figure 6. Vertical motion reconstructions for Santa Maria Island with the "tectonic correction" on relevant sea-level tracers; reference eustatic curve is from Miller et al. (2005), with long-term smoothed sea-level curve (LOESS curve fitting) represented by solid black line. Horizontal bars correspond to 2σ uncertainty in the age; vertical bars correspond to the uncertainty in elevation (which reflects both the instrumental uncertainty in elevation determination and the uncertainty in the definition of a paleo–sea-level tracer). Vertical shaded columns correspond to the approximate time intervals of each volcanic stage in the evolution of the island. The elevation of the highest marine terrace was simply defined as being 220 ± 10 m and assigned an age between 3.7 and 3.2 Ma, its upper and lower age bounds. Note the uplift trend from ca. 3.5 to 0 Ma at ~60 m/m.y., following a subsidence trend of ~100 m/m.y. MIS 5e—marine oxygen isotope stage 5e.

coarse sediments to finer bioclastic sediments with a clear open-marine character (Serralheiro, 2003; Ávila et al., 2012, 2017). As the gradual destruction of the Anjos edifice progressed and the deposition of Touril complex continued, Santa Maria's edifice became a wide, shallow-water sandy shoal punctuated by occasional residual islets or Surtseyan cones; sporadic volcanic activity was entirely submarine in nature and was mostly concentrated in the eastern and southern part of the edifice (Ávila et al., 2012, 2017). This scenario is supported by the fact that the Touril complex forms an almost continuous belt that can be followed around the island (except on the eastern side, where it disappears below present sea level), and by the fact that thick submarine effusive products of the subsequent volcanic stage invariably cover this sequence. Moreover, it is also supported by the rich marine fossil record of the Touril complex, which includes bones of cetaceans (Estevens and Ávila, 2007; Ávila et al., 2015b), teeth of sharks (Ávila et al., 2012) and of bony fishes, coralline algae (e.g., rhodoliths; Meireles et al., 2013; Rebelo et al., 2014; Ávila et al., 2015a, 2015d, 2017), and a large spectrum of marine invertebrates, e.g., molluscs, echinoderms, bryozoans, foraminiferans, and crustaceans (e.g., Kirby et al., 2007; Madeira et al., 2011; Meireles et al., 2013; Rebelo et al., 2014; Ávila et al., 2015a, 2015d, 2017). The gentle present-day east dip of the Touril complex (and the unconformity at its base) may denote a slight eastward tilting of the island edifice, possibly owing to the off-centered loading of the Pico Alto volcanic edifice (see Fig. 2) or owing to posterior differential uplift. This stage in the island's evolution is extremely important for paleo- and neo-biogeographical studies because, probably, nearly all of the terrestrial species that had colonized the first island of Santa Maria must have disappeared when the island became a guyot.

The next stage in the evolution of Santa Maria is tied to the construction of the Pico Alto volcanic edifice, centered on the eastern side of the existing island edifice. This stage started at ca. 4.1 Ma and lasted up to ca. 3.5 Ma. Continuous exposures along the coastal cliffs of the island clearly show that the Pico Alto volcanic edifice began entirely submarine, eventually breaching sea level as the edifice grew and volcanic aggradation outpaced subsidence. Effectively, the Pico Alto volcanic succession consists of submarine volcanic sequences and submarine volcanic morphologies, which only pass to subaerial at higher elevations, as noted by previous authors. The fact that the passage zone of these sequences is generally at higher elevations with decreasing age confirms that subsidence began during the previous volcanic phase and continued throughout the period spanned by the emplacement of the Pico Alto edifice. The construction of this volcano seems to have been mostly centered along the NNW-SSE fissure-fed central range of Pico Alto, from which the edifice expanded, particularly to the west and east of this feature. The edifice's lateral growth was essentially sustained by the westward and eastward progradation of coastal lava deltas during a gradual relative sea-level rise driven by subsidence, as indicated by the numerous lava-fed delta structures superbly exposed along the island's coastline. While the westward progradation of lava-fed deltas took place over the existing shoals (leading to the juxtaposition of Pico Alto effusive delta sequences over the Touril marine sediments), their eastward progradation extended the edifice beyond the existing shelf edge, as suggested by the vertical extension and the steep dip of the foresets on the eastern effusive deltas (see Fig. 3H).

The geometry described here for the eastern part of the edifice is in stark contrast with that

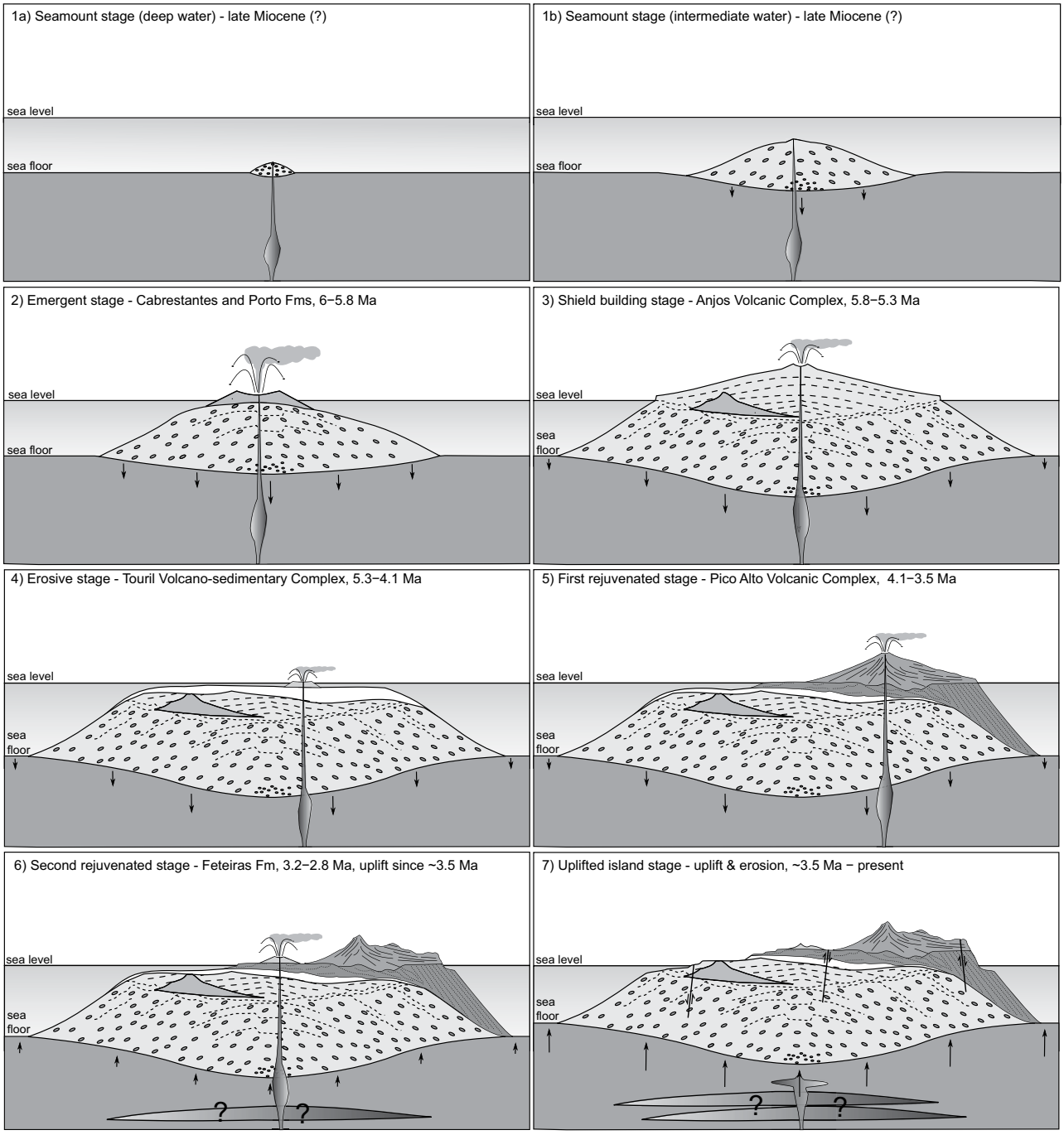

Figure 7. Sketch representing the main stages in the evolutionary history of Santa Maria Island. (1a) Seamount stage, deep-water substage, during the late Miocene (?): onset of island construction, initially as a largely effusive submarine volcano (inferred). (1b) Seamount stage, intermediate-water substage, during the late Miocene: sustained edifice growth by vigorous submarine effusive volcanism (inferred). (2) Emergent island stage, at ca. 6 Ma: first emergence above sea level by Surtseyan volcanism and transition to subaerial volcanism. (3) Shield-building stage, 5.7–5.3 Ma: sustained volcanism leading to the construction of a subaerial shield volcano, with accelerating subsidence. (4) Erosive stage, 5.3–4.3 Ma: waning volcanism, erosion, mass wasting (eventually including the loss of the eastern sector of the edifice), and subsidence, leading to truncation of the existing island edifice, and extensive marine sedimentation; the edifice probably resembled a wide sandy shoal by the end of this stage. (5) First rejuvenated stage, 4.1–3.5 Ma: renewed vigorous volcanism builds a new island edifice off-centered to the east of the old edifice, resulting in significant eastward and westward coastal advancement by progradation of lava-fed deltas, under continued subsidence; volcanic progradation to east overlapped existing shelf edge. (6) Second rejuvenated stage, 3.2–2.8 Ma, uplift since ca. 3.5 Ma: waning volcanism and a reversal to an uplift trend resulting in erosion and the generation of marine terraces; sporadic low-volume monogenetic volcanism continued until 2.8 Ma. (7) Uplifted island stage, ca. 3.5 (or 2.8) Ma to the present: continuous uplift and erosion, with marine erosion particularly concentrated on the windward side, leading to the present-day topography.

inferred by Sibrant et al. (2015a), who suggested that the whole eastern flank of Pico Alto was removed by a large-scale flank collapse sometime between 3.9 and 3.6 Ma. The architecture of the lava-fed deltas exposed all around the island's coast precisely shows that the overall volcanic structure of eastern Santa Maria dips to the eastern quadrant, and therefore the eastern flank of the edifice is not all missing. Moreover, the late construction of extensive lava-fed deltas unconformably over a well-developed insular shelf on the eastern side of the island, such as in Ponta do Norte, at ca. 3.5 Ma (Fig. 3G), shows that eastward/northward volcanic progradation was occurring until late in the evolution of the island edifice. This would not be the case if the eastern flank of the island had collapsed before 3.6 Ma. The hypothesis for a major flank collapse to have affected the Pico Alto volcanic edifice is therefore not supported by our observations and consequently not taken into account in this reconstruction.

The subsequent evolutionary stage in the evolution of Santa Maria is characterized by waning volcanism, erosion, and uplift (Fig. 7). The end of the Pico Alto volcanic phase is poorly constrained, but it possibly took place at around 3.7–3.5 Ma. During this period, volcanism shifted gradually from larger fissure-fed eruptions (which had sustained the growth of the edifice and the expansion of coastlines) to smaller monogenetic eruptions, punctuating the island edifice with low-volume magmatic and hydromagmatic cones and associated effusive products (e.g., Pico Maloás at Malbusca, Pico do Facho, Ponta do Norte cone, etc.). As volcanic growth waned and became more episodic, erosion increased topographic decay and coastal retreat. Coastal retreat was particularly pronounced on the western (windward) side of the island, leading to the formation of broad shelves that became marine terraces as the island was gradually uplifted. Episodic posterosional monogenetic volcanism of the Feteiras Formation continued up to 2.8 Ma (Sibrant et al. 2015a), partially covering the recently formed higher marine terraces with its products. The late Pliocene therefore marks the end of Santa Maria's volcanic life. However, following the cessation of volcanism, the island continued to experience uplift until the present day, as attested by the staircase of marine terraces that characterize the morphology of its western slope. This final stage in the island evolution was also accompanied by minor faulting accommodated by NNW-SSE (and more rarely NE-SW), nearly vertical, dip-slip block faulting, which displaced some of the higher marine terraces (Madeira, 1986; Madeira et al., 2015).

Coastal Evolution and Marine Terrace Development

We attribute the preferential development of broad marine terraces on the western side of Santa Maria to a combination of two main factors: stronger marine erosion on the windward side of the edifice, and a favorable lithological structure. The Azores Islands are shaped by a highly energetic wave regime dominantly approaching from the WNW due to the strong westerlies to which the archipelago is exposed (Quartau et al., 2010, 2012; Rusu and Soares, 2012). Marine erosion is therefore significantly stronger on the western and northern sides, partially explaining the existing asymmetry. Marine abrasion on the eastern side seems to have been much more limited, leading to the formation of plunging cliffs with occasional wave-cut notches, instead of coastal platforms; the very presence of wave-cut notches at different elevations precisely attests to the very low erosion rates affecting this side. The development of broad terraces on the western side may have also been facilitated by the fact that many of the terraces were carved along the softer Touril sequence and the gently dipping contacts between this unit and the underlying Anjos and overlying Pico Alto volcanic edifices. The extensive terraces located at elevations between 50 m and 120 m coincide precisely with those interfaces (cf. Figs. 2 and 4). Similarly, the generation of the extensive 210–230 m marine terrace was most likely facilitated by the presence of an antecedent flat morphology provided by the top of the western lava deltas of Pico Alto. Thus, we suggest that the staircase of marine terraces on the western side of the island is the fortuitous product of uplift, stronger marine erosion on the windward side, and a favorable lithological structure. In contrast, on the remaining coasts, the steepness of the plunging cliffs was sustained by low erosion rates (as the geometry of the MIS5e reconstructed shoreline also shows), possibly aided by small-scale mass wasting (rock and debris falls and topples on the steepest cliffs, and rockslides along the layered pillow and hyaloclastite slopes).

Possible Uplift Mechanisms

Santa Maria's long-lived uplift trend is quite remarkable, given the island's geodynamic setting. The island is located on very young lithosphere and therefore should be experiencing considerable thermal subsidence (Parsons and Sclater, 1977; Stein and Stein, 1992). In fact, practically all other Azorean Islands are clearly subsiding, including nearby São Miguel (Muecke et al., 1974; Trota, 2008; Catalão et al., 2011; Miranda et al., 2012, 2015; Marques et al., 2013). This subsidence probably results from the combined effects of recent volcanic loading (all other islands in the Azores are volcanically active and considerably younger than Santa Maria), thermal subsidence, and vertical displacement along regional tectonic structures (particularly São Miguel, Terceira, and Graciosa, which are located in the "central graben" of the Terceira ultraslow-spreading ridge). Given this regional context, the uplift trend at Santa Maria cannot be attributed to a regional, spatially broad mechanism, but rather to one that acts at a local scale.

A common uplift mechanism affecting several ocean-island systems involves the far-field flexural response of the lithosphere to younger volcanic loads, as has been shown to be the case of the Hawaiian chain and other Pacific archipelagos (e.g., Grigg and Jones, 1997; Zhong and Watts, 2002; Huppert et al., 2015). This mechanism, however, is not applicable to the case of Santa Maria because: (1) the only island edifice located at a reasonably suitable distance[2] to generate a flexural bulge capable of uplifting Santa Maria is the nearby island of São Miguel, which is considerably younger (<1 Ma; Johnson et al., 1998; Sibrant et al., 2015b) than the onset of uplift at Santa Maria; and (2) the magnitude of uplift is far too high to be explained by effects of flexural loading of a nearby island (Ramalho et al., 2010c; Huppert et al., 2015). Isostatic uplift or uplift generated by flexural rebound as result of erosion and mass wasting probably also accounts for only a small fraction of the uplift experienced by Santa Maria. While it is extremely difficult to quantify the amount of material removed by marine and fluvial erosion, it is reasonable to assume that this material was redistributed within the flexural moat of the edifice, diminishing considerably the possible uplift generated by the removal of material from the subaerial part of the island (Smith and Wessel, 2000). Additionally, the occurrence of large-scale mass wasting at the end of the Pico Alto volcanic phase (as proposed by Sibrant et al., 2015a) is not supported by the island's volcanic structure and therefore cannot account for the uplift reported here, despite a potential agreement between the proposed age for this hypothetical flank collapse and the onset of uplift. However, even if one accepts this hypothetical collapse, uplift following a catastrophic flank failure is expected to have been faster (e.g., see Smith and Wessel, 2000) than the slow uplift trend reported here, which extends over a period of 3.5 m.y.

[2]Considering an elastic plate model with flexural rigidity parameters compatible with thin oceanic lithosphere, or even considering a thickened plate due to the addition of the Azores Plateau.

Another possible uplift mechanism relates to the island's geotectonic setting. Santa Maria rises from the southeastern edge of the Azores Plateau, which is a triangular zone limited by the Terceira Rift to the NE, the East Azores fault zone and Princess Alice Rift to the SW, and the Glória fault to the SE (see Fig. 1). At ca. 4 Ma, the area experienced a tectonic reconfiguration due to the migration of the Eurasia-Nubian plate boundary from the incipient Princess Alice Rift to a location further north, now established as a diffuse plate boundary around the Terceira Rift (Miranda et al., 2015, 2017). The area where Santa Maria lies thus became wedged in between the major discontinuities that limit the Azores Plateau to the south and east and a developing spreading ridge to the NE. This reconfiguration, induced by the onset of the Terceira ultraslow-spreading ridge, could have resulted in localized uplift, acting to raise the island. However, neotectonic studies along the diffuse Azorean segment of the Eurasia-Nubian boundary point to a transtensional regime in the region, since all recognized active faults (both onshore and offshore) present normal or oblique (normal dextral or normal sinistral) slip (Madeira and Brum da Silveira, 2003; Hipólito et al., 2013; Carmo et al., 2013, 2015; Marques et al., 2013; Madeira et al., 2015; Trippanera et al., 2014). Such a regime is not compatible with significant tectonic uplift in this region.

In our opinion, Santa Maria's vertical motion history can only be explained by a gradual shift from a dominantly extrusive to a dominantly intrusive edifice growth process, resulting in uplift. This shift requires a localized change in the orientation of the prevailing minimum compressive stress (σ_3) from horizontal to vertical, resulting in preferential sill/laccolith intrusion rather than dike propagation to the surface (Ménand, 2008). The reasons behind this change are still poorly understood but may be related to stress rotation induced by earlier magmatic intrusions and/or waning magma pressures that caused σ_2 (vertical) to become σ_3 (Roman et al., 2004; Ménand, 2008). In order to generate uplift largely uncompensated by surface loading, a significant portion of these intrusions would need to have been emplaced at deep crustal levels and/or within the upper mantle. Moreover, they would need to be restricted to the island's footprint; otherwise, they would generate flexural uplift over a wider region, a feature not observed in this case.

Using a simple Airy isostatic model, we estimate that ~600 m of underplating/crustal thickening would be required to produce ~200 m of uplift (using ρ_{water} = 1030 kg m^{-3}, ρ_{load} = 2700 kg m^{-3}, and ρ_{mantle} = 3270 kg m^{-3}). This equates to an underplated/intruded volume of ~225 km^3 (assuming accumulation restricted to the island's footprint) emplaced over a span of ~3.5 m.y., yielding a magma production rate of ~8×10^{-5} km^3 yr^{-1}. Such a rate is well within the 5×10^{-5} to 1×10^{-1} km^3 yr^{-1} oceanic hotspot average (White et al., 2006) and is also of the same order of magnitude as the ~1.2×10^{-5} km^3 yr^{-1} estimated for the Pico Alto volcanic phase (using a subaerial volume of ~17 km^3 erupted over ~1.4 m.y.), attesting to the plausibility of our calculations.

Ample geological evidence exists for magmatic intrusions contributing to volcano growth through uplift, at various time scales and in different geodynamic settings. Resurgence at large collapse calderas is perhaps the better-documented case. It consists of surface uplift likely induced by repeated intrusions of sills, laccolith, and/or cryptodomes (or by the replenishment of shallow magma reservoirs), caused by a similar shift from dominantly extrusive to dominantly intrusive processes (Kennedy et al., 2012). Episodes of caldera resurgence have also been reported at varying time scales, from short multiple-month or year periods (e.g., Amelung et al., 2000; Chadwick et al., 2006; Chang et al., 2010) to longer 10^3–10^5 yr trends (e.g., Fridrich et al., 1991; Carlino et al., 2006). The process reported here, however, involves pronounced uplift at a volcanic edifice scale, likely driven by deep endogenous growth over longer time scales. Such a process has been shown to be the most likely cause for uplift at other Atlantic islands, namely, La Palma and El Hierro in the Canary Islands (Klügel et al., 2005, 2015), Santiago, São Nicolau, Brava, and Maio in the Cape Verdes (Ramalho et al., 2010a, 2010b, 2010c; Madeira et al., 2010), and Madeira Island in the Madeira Archipelago (Ramalho et al., 2015), all of which sit on old, thick lithosphere and within the slow-moving Nubian plate. In this setting, the slow motion of the plate (with respect to the melting source) combined with a thick lithosphere over the hotspot has been proposed as a factor that promoted endogenous growth over surface volcanism at geological time scales (Ramalho et al., 2015). The uplift trend at Santa Maria, however, shows that intrusive processes and endogenous island edifice growth may still play a significant role in ocean-island systems located on young lithosphere and at interplate settings such as the Azores.

CONCLUSIONS

In this study, we reconstructed the timing and magnitude of vertical displacement of Santa Maria Island in the Azores. Santa Maria is located in a geodynamic setting where a clear subsidence trend should be expected, but our data revealed a complex evolutionary history spanning ~6 m.y., with pronounced subsidence until ca. 3.5 Ma, followed by an uplift trend that extends to the present. This study was also the first to constrain the exact time of emergence for this island, the oldest in the archipelago.

Santa Maria Island first emerged by Surtseyan activity at ca. 6 Ma. Increased volcanism sustained the transition from emergent island stage to the subaerial shield stage, consolidating the island edifice and assuring its survival above sea level. This transition was characterized by a gradual shift from monogenetic volcanism to polygenetic shield volcanism, culminating with the formation of a broad shield volcano at around 5.8–5.3 Ma. It was also around this time that the edifice entered a pronounced subsidence trend that was to last up to ca. 3.5 Ma. The following stage in the evolution of the island edifice corresponds to an erosional stage characterized by topographical decay, subsidence, and marine sedimentation, with occasional low-volume submarine volcanism. This stage lasted until ca. 4.1 Ma, eventually leading to a partial or, more probably, almost complete truncation of the existing volcanic edifice, which at that time resembled a wide sandy shoal punctuated by occasional residual or juvenile (Surtseyan) islets. With renewed volcanism, the edifice eventually emerged again above sea level at ca. 4.1 Ma, this time essentially concentrated on the eastern side of the previous edifice. Sustained volcanic activity lasted until ca. 3.5 Ma, leading to considerable lateral growth by progradation of coastal lava-fed deltas, as subsidence progressed. At ca. 3.5 Ma, however, the island experienced a major change in its evolution, characterized by waning volcanism (lasting up to 2.8 Ma), gradual erosion, and a reversal to an uplift trend. This trend extended to the present, resulting in over 200 m of uplift and leading to the generation of a series of marine terraces on the windward side. It is precisely this uplift trend that is responsible for the exposure of superb volcanic and sedimentary marine sequences along Santa Maria's coastal cliffs, which make this island so famous amongst the Azores Archipelago.

The fact that an island located in this particular geotectonic context experienced such a pronounced uplift trend is remarkable and raises important questions concerning possible uplift mechanisms. Our analyses suggest that only one plausible uplift mechanism may account for Santa Maria's reversal from the expected subsidence trend to a long-term uplift trend: localized uplift as a result of a shift from dominantly extrusive to dominantly intrusive edifice growth, accompanied by crustal thickening. Further research is therefore necessary to investigate the island's crust and upper mantle in order to confirm the proposed crustal thickening.

ACKNOWLEDGMENTS

This work resulted from the project "Investigation of Island Uplift of the Azores Island Region" (TH1530/6-1) funded by The German Research Foundation (DFG), in collaboration with PTDC/GEO-GEO/0051/2014 PLATMAR, funded by Fundação para a Ciência e Tecnologia. R. Ramalho acknowledges his FP7-PEOPLE-2011-IOF Marie Curie Fellowship. A. Rovere's research was supported by the Institutional Strategy of the University of Bremen, funded by the German Excellence Initiative (ABPZuK-03/2014) and by the Center for Tropical Marine Ecology (ZMT). Publication supported by FCT-project UID/GEO/50019/2013—Instituto Dom Luiz. We also kindly acknowledge the following persons and institutions for all the support given during the course of this work: The regional government of the Azores; R. Câmara, J. Bairos, N. Moura, and J. Pombo of Serviços de Ambiente da Ilha de Santa Maria, for all the support in the field; Clube Naval de Santa Maria and particularly our skipper M. Cabral for numerous boat trips to study the island; M. Antunes at Secretaria Regional do Turismo e Transportes for providing the digital altimetric database and aerial photo coverage used in this study; our colleagues at the Instituto de Investigação em Vulcanologia e Avaliação de Riscos (IVAR), University of Azores, for their kind support; SATA Air Azores for facilitating the transportation of equipment and samples; and finally, but not the least, all the participants of the several international workshops "Palaeontology in Atlantic Islands," who over the years (2009–2014) participated in the field work, in particular, C. Rebelo, C. Melo, P. Madeira, R. Cordeiro, and R. Meireles. We also thank M. Miranda for the helpful discussion about the evolution of the Azores triple junction. Finally, we would like to thank D. Geist, A. Klüguel, V. Acocella (reviewers), J. Colgan (U.S. Geological Survey internal reviewer), Associate Editor Luca Ferrari, and Editor Brad Singer for insightful comments that helped to improve this manuscript. Any use of trade, product, or firm names is for descriptive purposes only and does not imply endorsement by the U.S. government.

REFERENCES CITED

Abdel-Monem, A., Fernandez, L., and Boone, G., 1975, K-Ar ages from the eastern Azores group (Santa Maria, São Miguel and the Formigas islands): Lithos, v. 8, no. 4, p. 247–254, doi:10.1016/0024-4937(75)90008-0.

Agostinho, J., 1931, The volcanoes of the Azores Islands: Bulletin of Volcanology, v. 8, no. 1, p. 123–138, doi:10.1007/BF02720216.

Ali, M.Y., Watts, A.B., and Hill, I., 2003, A seismic reflection profile study of lithospheric flexure in the vicinity of the Cape Verde Islands: Journal of Geophysical Research–Solid Earth, v. 108, no. B5, p. 2239–2263.

Amelung, F., Jónsson, S., Zebker, H. and Segall, P., 2000, Widespread uplift and 'trapdoor' faulting on Galapagos volcanoes observed with radar interferometry: Nature, v. 407(6807), p. 993–996.

Asimow, P.D., Dixon, J.E., and Langmuir, C.H., 2004, A hydrous melting and fractionation model for mid-ocean ridge basalts: Application to the Mid-Atlantic Ridge near the Azores: Geochemistry Geophysics Geosystems, v. 5, no. 1, p. Q01E16, doi:10.1029/2003GC000568.

Ávila, S.P., Madeira, P., Da Silva, C.M., Cachão, M., Landau, B., Quartau, R., and Martins, A.M., 2008, Local disappearance of bivalves in the Azores during the last glaciation: Journal of Quaternary Science, v. 23, no. 8, p. 777–785, doi:10.1002/jqs.1165.

Ávila, S.P., Madeira, P., Zazo, C., Kroh, A., Kirby, M., da Silva, C.M., Cachão, M., and Frias Martins, A.M., 2009, Palaeoecology of the Pleistocene (MIS 5.5) outcrops of Santa Maria Island (Azores) in a complex oceanic tectonic setting: Palaeogeography, Palaeoclimatology, Palaeoecology, v. 274, no. 1–2, p. 18–31, doi:10.1016/j.palaeo.2008.12.014.

Ávila, S.P., Ramalho, R.S., and Vullo, R., 2012, Systematics, palaeoecology and palaeobiogeography of the Neogene fossil sharks from the Azores (northeast Atlantic): Annales de Paléontologie, v. 98, no. 3, p. 167–189, doi:10.1016/j.annpal.2012.04.001.

Ávila, S.P., Cachão, M., Ramalho, R.S., Botelho, A.Z., Madeira, P., Rebelo, A.C., Cordeiro, R., Melo, C., Hipólito, A., Ventura, M.A., and Lipps, J.H., 2015a, The palaeontological heritage of Santa Maria Island (Azores: NE Atlantic): A re-evaluation of geosites in GeoPark Azores and their use in geotourism: Geoheritage, v. 8, no. 2, p. 155–171.

Ávila, S.P., Cordeiro, R., Rodrigues, A.R., Rebelo, A.C., Melo, C., Madeira, P., and Pyenson, N.D., 2015b, Fossil Mysticeti from the Pleistocene of Santa Maria Island, Azores (NE Atlantic Ocean), and the prevalence of fossil cetaceans on oceanic islands: Palaeontologia Electronica, v. 18.2.27A, p. 1–12, palaeo-electronica.org/content/2015/1225-oceanic-island-fossil-cetacean (accessed 2015).

Ávila, S.P., Melo, C., Silva, L., Ramalho, R.S., Quartau, R., Hipólito, A., Cordeiro, R., Rebelo, A.C., Madeira, P., Rovere, A., and Hearty, P.J., 2015c, A review of the MIS 5e highstand deposits from Santa Maria Island (Azores, NE Atlantic): Palaeobiodiversity, palaeoecology and palaeobiogeography: Quaternary Science Reviews, v. 114, p. 126–148, doi:10.1016/j.quascirev.2015.02.012.

Ávila, S.P., Ramalho, R.S., Habermann, J.M., Quartau, R., Kroh, A., Berning, B., Johnson, M., Kirby, M.X., Zanon, V., Titschack, J., Goss, A., Rebelo, A.C., Melo, C., Madeira, P., Cordeiro, R., Bagaço, L., Hipólito, A., Johnson, M., Uchman, A., Marques da Silva, C., Cachão, M., and Madeira, J., 2015d, Palaeoecology, taphonomy, and preservation of a Lower Pliocene shell bed (coquina) from a volcanic oceanic island (Santa Maria Island, Azores): Palaeogeography, Palaeoclimatology, Palaeoecology, v. 430, p. 57–73, doi:10.1016/j.palaeo.2015.04.015.

Ávila, S.P., Ramalho, R.S., and Titschack, J., 2017, The marine fossil record at Santa Maria Island (Azores), *in* Küppers, U., and Beier, C., eds., Volcanoes of the Azores. Active Volcanoes of the World: Berlin, Germany, Springer Verlag (in press).

Beier, C., Haase, K.M., and Turner, S.P., 2012, Conditions of melting beneath the Azores: Lithos, v. 144–145, p. 1–11, doi:10.1016/j.lithos.2012.02.019.

Beier, C., Mata, J., Stöckhert, F., Mattielli, N., Brandl, P.A., Madureira, P., Genske, F.S., Martins, S., Madeira, J., and Haase, K.M., 2013, Geochemical evidence for melting of carbonated peridotite on Santa Maria Island, Azores: Contributions to Mineralogy and Petrology, v. 165, no. 5, p. 823–841, doi:10.1007/s00410-012-0837-2.

Bonatti, E., 1990, Not so hot "hot spots" in the oceanic mantle: Science, v. 250, no. 4977, p. 107–111, doi:10.1126/science.250.4977.107.

Burke, K., and Wilson, J., 1972, Is the African plate stationary?: Nature, v. 239, no. 5372, p. 387–390, doi:10.1038/239387b0.

Carlino, S., Cubellis, E., Luongo, G., and Obrizzo, F., 2006, On the mechanics of caldera resurgence of Ischia Island (southern Italy), *in* Troise, C., de Natale, G., and Kilburn, C.R.J., eds., Mechanisms of Activity and Unrest at Large Calderas: Geological Society of London Special Publication 269, p. 181–193, doi:10.1144/GSL.SP.2006.269.01.12.

Carmo, R., Madeira, J., Hipólito, A., and Ferreira, T., 2013, Paleoseismological evidence for historical surface rupture in S. Miguel Island (Azores): Annals of Geophysics, v. 56, no. 6, p. S0671.

Carmo, R., Madeira, J., Ferreira, T., Queiroz, G., and Hipólito, A., 2015, Volcano-tectonic structures of S. Miguel Island, *in* Gaspar, J.L., Guest, J.E., Duncan, A.M., Barriga, F.J.A.S., and Chester, D.K., eds., Volcanic Geology of São Miguel Island (Azores Archipelago): Geological Society of London Memoir 44, p. 65–86.

Cas, R., and Wright, J., 1987, Volcanic Successions. Modern and Ancient: A Geological Approach to Processes, Products and Successions: London, Chapman & Hall, 528 p., doi:10.1007/978-94-009-3167-1.

Catalão, J.C., Nico, G., Hanssen, R., and Catita, C., 2011, Merging GPS and atmospherically corrected InSAR data to map 3-D terrain displacement velocity: IEEE (Institute of Electrical and Electronics Engineers) Transactions on Geoscience and Remote Sensing, v. 49, no. 6, p. 2354–2360.

Chadwick, W.W., Geist, D.J., Jónsson, S., Poland, M., Johnson, D.J., and Meertens, C.M., 2006, A volcano bursting at the seams: Inflation, faulting, and eruption at Sierra Negra Volcano, Galápagos: Geology, v. 34, no. 12, p. 1025–1028, doi:10.1130/G22826A.1.

Chang, W.L., Smith, R.B., Farrell, J., and Puskas, C.M., 2010, An extraordinary episode of Yellowstone caldera uplift, 2004–2010, from GPS and InSAR observations: Geophysical Research Letters, v. 37, no. 23, p. L23302, doi:10.1029/2010GL045451.

Creveling, J.R., Mitrovica, J.X., Hay, C.C., Austermann, J., and Kopp, R.E., 2015, Revisiting tectonic corrections applied to Pleistocene sea-level highstands: Quaternary Science Reviews, v. 111, p. 72–80, doi:10.1016/j.quascirev.2015.01.003.

Dalrymple, G.B., Alexander, E.C., Lanphere, M.A., and Kraker, G.P., 1981, Irradiation of Samples for $^{40}Ar/^{39}Ar$ Dating Using the Geological Survey TRIGA Reactor: U.S. Geological Survey Professional Paper 1176, 62 p.

Dutton, A., and Lambeck, K., 2012, Ice volume and sea level during the last interglacial: Science, v. 337, no. 6091, p. 216–219, doi:10.1126/science.1205749.

Estevens, M., and Ávila, S.P., 2007, Fossil whales from the Azores: Açoreana, v. 5, p. 140–161.

Féraud, G., Kaneoka, I., and Allègre, C.J., 1980, K/Ar ages and stress pattern in the Azores: Geodynamic implications: Earth and Planetary Science Letters, v. 46, no. 2, p. 275–286, doi:10.1016/0012-821X(80)90013-8.

Féraud, G., Gastaud, J., Schmincke, H., Pritchard, G., Lietz, J., and Bleil, U., 1981, New K-Ar ages, chemical analyses and magnetic data of rocks from the islands of Santa Maria (Azores), Porto Santo and Madeira (Madeira Archipelago) and Gran Canaria (Canary Islands): Bulletin of Volcanology, v. 44, no. 3, p. 359–375, doi:10.1007/BF02600570.

Fernandes, R.M.S., Bastos, L., Miranda, J.M., Lourenço, N., Ambrosius, B.A.C., Noomen, R., and Simons, W., 2006, Defining the plate boundaries in the Azores region: Journal of Volcanology and Geothermal Research, v. 156, no. 1–2, p. 1–9, doi:10.1016/j.jvolgeores.2006.03.019.

Fridrich, C.J., Smith, R.P., DeWitt, E.D., and McKee, E.H., 1991, Structural, eruptive, and intrusive evolution of the Grizzly Peak caldera, Sawatch Range, Colorado: Geological Society of America Bulletin, v. 103, no. 9, p. 1160–1177, doi:10.1130/0016-7606(1991)103<1160:SEAIEO>2.3.CO;2.

Gente, P., Dyment, J., Maia, M., and Goslin, J., 2003, Interaction between the Mid-Atlantic Ridge and the Azores hotspot during the last 85 Myr: Emplacement and rifting of the hot spot–derived plateaus: Geochemistry Geophysics Geosystems, v. 4, no. 10, p. 8514, doi:10.1029/2003GC000527.

Grigg, R., and Jones, A., 1997, Uplift caused by lithospheric flexure in the Hawaiian Archipelago as revealed by elevated coral deposit: Marine Geology, v. 141, no. 1–4, p. 11–25, doi:10.1016/S0025-3227(97)00069-8.

Hearty, P.J., Hollin, J.T., Neumann, A.C., O'Leary, M.J., and McCulloch, M., 2007, Global sea-level fluctuations during the last interglaciation (MIS 5e): Quaternary Science Reviews, v. 26, p. 2090–2112, doi:10.1016/j.quascirev.2007.06.019.

Hipólito, A., Madeira, J., Carmo, R., and Gaspar, J.L., 2013, Neotectonics of Graciosa Island (Azores): A contribution to seismic hazard assessment of a volcanic area in a complex geodynamic setting: Annals of Geophysics, v. 56, no. 6, p. S0677.

Huppert, K.L., Royden, L.H., and Perron, J.T., 2015, Dominant influence of volcanic loading on vertical motions of the Hawaiian Islands: Earth and Planetary Science Letters, v. 418, p. 149–171, doi:10.1016/j.epsl.2015.02.027.

Janssen, A.W., Kroh, A., and Ávila, S.P., 2008, Early Pliocene heteropods and pteropods (Mollusca, Gastropoda) from Santa Maria (Azores, Portugal): Systematics and biostratigraphic implications: Acta Geologica Polonica, v. 58, p. 355–369.

Johnson, C.L., Wijbrans, J.R., Constable, C.G., Gee, J., Staudigel, H., Tauxe, L., Forjaz, V.-H., and Salgueiro, M., 1998, $^{40}Ar/^{39}Ar$ ages and paleomagnetism of São Miguel lavas, Azores: Earth and Planetary Science Letters, v. 160, no. 3–4, p. 637–649, doi:10.1016/S0012-821X(98)00117-4.

Jones, J., and Nelson, P., 1970, The flow of basalt lava from air into water, its structural expression and stratigraphic significance: Geological Magazine, v. 107, no. 1, p. 13–19, doi:10.1017/S0016756800054649.

Kennedy, B., Wilcock, J., and Stix, J., 2012, Caldera resurgence during magma replenishment and rejuvenation at Valles and Lake City calderas: Bulletin of Volcanology, v. 74, no. 8, p. 1833–1847, doi:10.1007/s00445-012-0641-x.

Kirby, M.X., Jones, D.S., and Ávila, S.P., 2007, Neogene shallow-marine paleoenvironments and preliminary strontium isotope chronostratigraphy of Santa Maria Island, Azores: Açoreana, v. 5, p. 112–125.

Klügel, A., Hansteen, T., and Galipp, K., 2005, Magma storage and underplating beneath Cumbre Vieja volcano, La Palma (Canary Islands): Earth and Planetary Science Letters, v. 236, no. 1–2, p. 211–226, doi:10.1016/j.epsl.2005.04.006.

Klügel, A., Longpré, M.-A., García-Cañada, L., and Stix, J., 2015, Deep intrusions, lateral magma transport and related uplift at ocean island volcanoes: Earth and Planetary Science Letters, v. 431, p. 140–149, doi:10.1016/j.epsl.2015.09.031.

Kopp, R.E., Simons, F.J., Mitrovica, J.X., Maloof, A.C., and Oppenheimer, M., 2009, Probabilistic assessment of sea level during the last interglacial stage: Nature, v. 462, no. 7275, p. 863–867, doi:10.1038/nature08686.

Krause, D.C., and Watkins, N.D., 1970, North Atlantic crustal genesis in the vicinity of the Azores: Geophysical Journal International, v. 19, no. 3, p. 261–283, doi:10.1111/j.1365-246X.1970.tb06046.x.

Kuiper, K., Deino, A., Hilgen, F., Krijgsman, W., Renne, P., and Wijbrans, J., 2008, Synchronizing rock clocks of Earth history: Science, v. 320, no. 5875, p. 500–504, doi:10.1126/science.1154339.

Laughton, A.S., and Whitmarsh, R.B., 1974, The Azores-Gibraltar plate boundary, *in* Kristjansson, L., ed., Geodynamics of Iceland and the North Atlantic Area: Dordrecht, Netherlands, D. Reidel Publishing Co., p. 63–81, doi:10.1007/978-94-010-2271-2_5.

Lee, J.-Y., Marti, K., Severinghaus, J.P., Kawamura, K., Yoo, H.-S., Lee, J.B., and Kim, J.S., 2006, A redetermination of the isotopic abundances of atmospheric Ar: Geochimica et Cosmochimica Acta, v. 70, no. 17, p. 4507–4512, doi:10.1016/j.gca.2006.06.1563.

Lourenço, N., Miranda, J.M., Luís, J.F., Ribeiro, A., Victor, L.M., Madeira, J., and Needham, H., 1998, Morphotectonic analysis of the Azores Volcanic Plateau from a new bathymetric compilation of the area: Marine Geophysical Researches, v. 20, no. 3, p. 141–156, doi:10.1023/A:1004505401547.

Luís, J.F., and Miranda, J.M., 2008, Reevaluation of magnetic chrons in the North Atlantic between 35°N and 47°N: Implications for the formation of the Azores triple junction and associated plateau: Journal of Geophysical Research–Solid Earth (1978–2012), v. 113, no. B10, p. B10105, doi:10.1029/2007JB005573.

Luís, J.F., Miranda, J.M., Galdeano, A., Patriat, P., Rossignol, J.C., and Mendes Victor, L.A., 1994, The Azores triple junction evolution since 10 Ma from an aeromagnetic survey of the Mid-Atlantic Ridge: Earth and Planetary Science Letters, v. 125, p. 439–459, doi:10.1016/0012-821X(94)90231-3.

Madeira, J., 1986, Geologia Estrutural e Enquadramento Geotectónico da Ilha de Santa Maria (Açores) [M.S. thesis]: Lisbon, Portugal, Universidade de Lisboa, 107 p.

Madeira, J., and Brum da Silveira, A., 2003, Active tectonics and first paleoseismological results in Faial, Pico and S. Jorge islands (Azores, Portugal): Annals of Geophysics, v. 46, no. 5, p. 733–761.

Madeira, J., and Ribeiro, A., 1990, Geodynamic models for the Azores triple junction: A contribution from tectonics: Tectonophysics, v. 184, no. 3–4, p. 405–415, doi:10.1016/0040-1951(90)90452-E.

Madeira, J., Mata, J., Mourão, C., Brum da Silveira, A., Martins, S., Ramalho, R.S., and Hoffmann, D., 2010, Volcano-stratigraphic and structural evolution of Brava Island (Cape Verde) from $^{40}Ar/^{39}Ar$, U/Th and field constraints: Journal of Volcanology and Geothermal Research, v. 196, no. 3–4, p. 219–235, doi:10.1016/j.jvolgeores.2010.07.010.

Madeira, P., Kroh, A., Cordeiro, R., Meireles, R., and Ávila, S.P., 2011, The fossil echinoids of Santa Maria Island, Azores (northern Atlantic Ocean): Acta Geologica Polonica, v. 61, p. 243–264.

Madeira, J., Brum da Silveira, A., Hipólito, A., and Carmo, R., 2015, Active tectonics along the Eurasia-Nubia boundary: Data from the central and eastern Azores Islands, *in* Gaspar, J.L., Guest, J.E., Duncan, A.M., Barriga, F.J.A.S., and Chester, D.K., eds., Volcanic Geology of São Miguel Island (Azores Archipelago): Geological Society of London Memoir 44, p. 15–32.

Madureira, P., Moreira, M., Mata, J., and Allégre, C.J., 2005, Primitive neon isotopes in Terceira Island (Azores archipelago): Earth and Planetary Science Letters, v. 233, no. 3–4, p. 429–440, doi:10.1016/j.epsl.2005.02.030.

Marques, F.O., Catalão, J.C., DeMets, C., Costa, A.C.G., and Hildenbrand, A., 2013, GPS and tectonic evidence for a diffuse plate boundary at the Azores triple junction: Earth and Planetary Science Letters, v. 381, p. 177–187, doi:10.1016/j.epsl.2013.08.051.

McNutt, M., and Menard, H.W., 1978, Lithospheric flexure and uplifted atolls: Journal of Geophysical Research–Solid Earth, v. 83, no. B3, p. 1206–1212, doi:10.1029/JB083iB03p01206.

Meireles, R.P., Quartau, R., Ramalho, R.S., Rebelo, A.C., Madeira, J., Zanon, V., and Ávila, S.P., 2013, Depositional processes on oceanic island shelves—Evidence from storm-generated Neogene deposits from the mid-North Atlantic: Sedimentology, v. 60, no. 7, p. 1769–1785, doi:10.1111/sed.12055.

Ménand, T., 2008, The mechanics and dynamics of sills in layered elastic rocks and their implications for the growth of laccoliths and other igneous complexes: Earth and Planetary Science Letters, v. 267, no. 1–2, p. 93–99, doi:10.1016/j.epsl.2007.11.043.

Menard, H., 1983, Insular erosion, isostasy, and subsidence: Science, v. 220, no. 4600, p. 913–918, doi:10.1126/science.220.4600.913.

Menéndez, I., Silva, P., Martin-Betancor, M., Perez-Torrado, F., Guillou, H., and Scaillet, S., 2008, Fluvial dissection, isostatic uplift, and geomorphological evolution of volcanic islands (Gran Canaria, Canary Islands, Spain): Geomorphology, v. 102, no. 1, p. 189–203, doi:10.1016/j.geomorph.2007.06.022.

Métrich, N., Zanon, V., Créon, L., Hildenbrand, A., Moreira, M., and Marques, F.O., 2014, Is the 'Azores hotspot' a wetspot? Insights from the geochemistry of fluid and melt inclusions in olivine of Pico basalts: Journal of Petrology, v. 55, no. 2, p. 377–393, doi:10.1093/petrology/egt071.

Miller, K., Kominz, M., Browning, J., Wright, J., Mountain, G., Katz, M., Sugarman, P., Cramer, B., Christie-Blick, N., and Pekar, S., 2005, The Phanerozoic record of global sea-level change: Science, v. 310, no. 5752, p. 1293–1298, doi:10.1126/science.1116412.

Min, K., Mundil, R., Renne, P.R., and Ludwig, K.R., 2000, A test for systematic errors in $^{40}Ar/^{39}Ar$ geochronology through comparison with U/Pb analysis of a 1.1-Ga rhyolite: Geochimica et Cosmochimica Acta, v. 64, no. 1, p. 73–98, doi:10.1016/S0016-7037(99)00204-5.

Miranda, J.M., Navarro, A., Catalão, J., and Fernandes, R.M.S., 2012, Surface displacement field at Terceira Island deduced from repeated GPS measurements: Journal of Volcanology and Geothermal Research, v. 217–218, p. 1–7, doi:10.1016/j.jvolgeores.2011.10.009.

Miranda, J.M., Luís, J.F., Lourenço, N., and Fernandes, R.M.S., 2015, The structure of the Azores triple junction: Implications for São Miguel Island, *in* Gaspar, J.L., Guest, J.E., Duncan, A.M., Barriga, F.J.A.S., and Chester, D.K., eds., Volcanic Geology of São Miguel Island (Azores Archipelago): Geological Society of London Memoir 44, p. 5–13, doi:10.1144/M44.2.

Miranda, J.M., Luís, J.F., and Lourenço, N., 2017, The geophysical architecture of the Azores from magnetic data, *in* Küppers, U., and Beier, C., eds., Volcanoes of the Azores. Active Volcanoes of the World: Berlin, Springer Verlag (in press).

Moore, J., 1970, Relationship between subsidence and volcanic load, Hawaii: Bulletin of Volcanology, v. 34, no. 2, p. 562–576, doi:10.1007/BF02596771.

Morgan, J., Morgan, W., and Price, E., 1995, Hotspot melting generates both hotspot volcanism and a hotspot swell: Journal of Geophysical Research–Solid Earth, v. 100, no. B5, p. 8045–8062, doi:10.1029/94JB02887.

Muecke, G.K., Ade-Hall, J.M., Aumento, F., MacDonald, A., and Reynolds, P.H., 1974, Deep drilling in an active geothermal area in the Azores: Nature, v. 252, p. 281–285, doi:10.1038/252281a0.

O'Leary, M.J., Hearty, P.J., Thompson, W.G., Mitrovica, J.X., Raymo, M.E., and Webster, J.M., 2013, Ice sheet collapse following a prolonged period of stable sea level during the last interglacial: Nature Geoscience, v. 6, no. 9, p. 796–800, doi:10.1038/ngeo1890.

Parsons, B., and Sclater, J., 1977, An analysis of the variation of ocean floor bathymetry and heat flow with age: Journal of Geophysical Research–Solid Earth, v. 82, no. 5, p. 803–827, doi:10.1029/JB082i005p00803.

Porębski, S., and Gradziński, R., 1990, Lava-fed Gilbert-type delta in the Polonez Cove Formation (Lower Oligocene), King George Island, West Antarctica, *in* Colella, A., and Prior, D., eds., Coarse Grained Deltas: International Association of Sedimentologists Special Publication 10, p. 333–351, doi:10.1002/9781444303858.ch19.

Quartau, R., Trenhaile, A.S., Mitchell, N.C., and Tempera, F., 2010, Development of volcanic insular shelves: Insights from observations and modelling of Faial Island in the Azores Archipelago: Marine Geology, v. 275, no. 1–4, p. 66–83, doi:10.1016/j.margeo.2010.04.008.

Quartau, R., Tempera, F., Mitchell, N.C., Pinheiro, L.M., Duarte, H., Brito, P.O., Bates, R., and Monteiro, J.H., 2012, Morphology of the Faial Island shelf (Azores): The interplay between volcanic, erosional, depositional, tectonic and mass-wasting processes: Geochemistry Geophysics Geosystems, v. 13, p. Q04012, doi:10.1029/2011GC003987.

Quartau, R., Hipólito, A., Romagnoli, C., Casalbore, D., Madeira, J., Tempera, F., Roque, C., and Chiocci, F.L., 2014, The morphology of insular shelves as a key for understanding the geological evolution of volcanic islands: Insights from Terceira Island (Azores): Geochemistry Geophysics Geosystems, v. 15, p. 1801–1826, doi:10.1002/2014GC005248.

Quartau, R., Madeira, J., Mitchell, N.C., Tempera, F., Silva, P.F., and Brandão, F., 2015, The insular shelves of the Faial-Pico Ridge: A morphological record of its geologic evolution (Azores archipelago): Geochemistry Geophysics Geosystems, v. 16, p. 1401–1420, doi:10.1002/2015GC005733.

Quartau, R., Madeira, J., Mitchell, N.C., Tempera, F., Silva, P.F., and Brandão, F., 2016, Reply to comment by Marques et al. on "The insular shelves of the Faial-Pico Ridge (Azores archipelago): A morphological record of its evolution": Geochemistry Geophysics Geosystems, v. 17, no. 2, p. 633–641, doi:10.1002/2015GC006180.

Ramalho, R.S., 2011, Building the Cape Verde Islands (1st ed.): Berlin, Springer, 207 p., doi:10.1007/978-3-642-19103-9.

Ramalho, R.S., Helffrich, G., Schmidt, D.N., and Vance, D., 2010a, Tracers of uplift and subsidence in the Cape Verde Archipelago: Journal of the Geological Society of London, v. 167, no. 3, p. 519–538, doi:10.1144/0016-76492009-056.

Ramalho, R.S., Helffrich, G., Cosca, M., Vance, D., Hoffmann, D., and Schmidt, D.N., 2010b, Episodic swell growth inferred from variable uplift of the Cape Verde hotspot islands: Nature Geoscience, v. 3, no. 11, p. 774–777, doi:10.1038/ngeo982.

Ramalho, R.S., Helffrich, G., Cosca, M., Vance, D., Hoffmann, D., and Schmidt, D.N., 2010c, Vertical movements of ocean island volcanoes: Insights from a

stationary plate environment: Marine Geology, v. 275, p. 84–95, doi:10.1016/j.margeo.2010.04.009.

Ramalho, R.S., Quartau, R., Trenhaile, A.S., Mitchell, N.C., Woodroffe, C.D., and Ávila, S.P., 2013, Coastal evolution on volcanic oceanic islands: A complex interplay between volcanism, erosion, sedimentation, sea-level change and biogenic production: Earth-Science Reviews, v. 127, p. 140–170, doi:10.1016/j.earscirev.2013.10.007.

Ramalho, R.S., Brum da Silveira, A., Fonseca, P.E., Madeira, J., Cosca, M., Cachão, M., Fonseca, M.M., and Prada, S.N., 2015, The emergence of volcanic oceanic islands on a slow-moving plate: The example of Madeira Island, NE Atlantic: Geochemistry Geophysics Geosystems, v. 16, no. 2, p. 522–537, doi:10.1002/2014GC005657.

Rebelo, A.C., Rasser, M.W., Riosmena-Rodriguez, R., and Ávila, S.P., 2014, Rhodolith forming coralline algae in the Upper Miocene of Santa Maria Island (Azores, NE Atlantic): A critical evaluation: Phytotaxa, v. 190, no. 1, p. 370–382, doi:10.11646/phytotaxa.190.1.22.

Rebelo, A.C., Rasser, M.W., Kroh, A., Johnson, M.E., Melo, C., Ramalho, R.S., Uchman, A., Zanon, V., Silva, L., Neto, A.I., Berning, B., Cachão, M., and Ávila, S.P., 2016, Rocking around a volcanic island shelf: Neogene rhodolith beds from Malbusca, Santa Maria Island (Azores, NE Atlantic): Facies, v. 62, no. 3, p. 1–31.

Roman, D.C., Moran, S.C., Power, J.A., and Cashman, K.V., 2004, Temporal and spatial variation of local stress fields before and after the 1992 eruptions of Crater Peak vent, Mount Spurr volcano, Alaska: Bulletin of the Seismological Society of America, v. 94, no. 6, p. 2366–2379, doi:10.1785/0120030259.

Rovere, A., Antonioli, F., and Bianchi, C.N., 2015, Fixed biological indicators, *in* Shennan, I., Long, A.J., and Horton, B.P., eds., Handbook of Sea-Level Research: Chichester, UK, Wiley, p. 268–280.

Rovere, A., Raymo, M.E., Vacchi, M., Lorscheid, T., Stocchi, P., Gómez-Pujol, L., Harris, D.L., Casella, E., O'Leary, M.J., and Hearty, P.J., 2016, The analysis of last interglacial (MIS 5e) relative sea-level indicators: Reconstructing sea-level in a warmer world: Earth-Science Reviews, v. 159, p. 404–427, doi:10.1016/j.earscirev.2016.06.006.

Rusu, L., and Soares, C.G., 2012, Wave energy assessments in the Azores islands: Renewable Energy, v. 45, p. 183–196, doi:10.1016/j.renene.2012.02.027.

Saki, M., Thomas, C., Nippress, S.E., and Lessing, S., 2015, Topography of upper mantle seismic discontinuities beneath the North Atlantic: The Azores, Canary and Cape Verde plumes: Earth and Planetary Science Letters, v. 409, p. 193–202, doi:10.1016/j.epsl.2014.10.052.

Schilling, J.-G., 1975, Azores mantle blob: Rare-earth evidence: Earth and Planetary Science Letters, v. 25, no. 2, p. 103–115, doi:10.1016/0012-821X(75)90186-7.

Schmidt, R., and Schmincke, H.-U., 2000, Seamounts and island building, *in* Sigurdsson, H., Houghton, B., McNutt, S., Rymer, H., and Stix, J., eds., Encyclopedia of Volcanoes: San Diego, California, Academic Press, p. 383–402.

Schmidt, R., and Schmincke, H.-U., 2002, From seamount to oceanic island, Porto Santo, central East-Atlantic: International Journal of Earth Sciences, v. 91, no. 4, p. 594–614, doi:10.1007/s00531-001-0243-x.

Searle, R., 1980, Tectonic pattern of the Azores spreading centre and triple junction: Earth and Planetary Science Letters, v. 51, no. 2, p. 415–434, doi:10.1016/0012-821X(80)90221-6.

Sepúlveda, P., Le Roux, J., Lara, L., Orozco, G., and Astudillo, V., 2015, Biostratigraphic evidence for dramatic Holocene uplift of Robinson Crusoe Island, Juan Fernandez Ridge, SE Pacific Ocean: Biogeosciences, v. 12, no. 6, p. 1993–2001, doi:10.5194/bg-12-1993-2015.

Serralheiro, A., 2003, A geologia da Ilha de Santa Maria, Açores: Açoreana, v. 10, no. 1, p. 141–192.

Serralheiro, A., Alves, C.A.M., Forjaz, V.H., and Rodrigues, B., 1987, Carta Vulcanológica dos Açores. Ilha de Santa Maria na (folhas 1 e 2): Ponta Delgada, Serviço Regional de Protecção Civil dos Açores, Universidade dos Açores and Centro de Vulcanologia, scale 1:15,000.

Serralheiro, A. and Madeira, J.M., 1990, Stratigraphy and geochronology of Santa Maria Island (Azores), *in* Livro de Homenagem a Carlos Romariz: Secção de Geologia Económica e Aplicada, Departamento de Geologia, FCUL, Lisboa, p. 357–376.

Sibrant, A.L.R., Hildenbrand, A., Marques, F.O., and Costa, A.C.G., 2015a, Volcano-tectonic evolution of the Santa Maria Island (Azores): Implications for paleostress evolution at the western Eurasia-Nubia plate boundary: Journal of Volcanology and Geothermal Research, v. 291, p. 49–62, doi:10.1016/j.jvolgeores.2014.12.017.

Sibrant, A.L.R., Hildenbrand, A., Marques, F.O., Weiss, B., Boulesteix, T., Hübscher, C., Lüdmann, T., Costa, A.C.G., and Catalão, J.C., 2015b, Morpho-structural evolution of a volcanic island developed inside an active oceanic rift: S. Miguel Island (Terceira Rift, Azores): Journal of Volcanology and Geothermal Research, v. 301, p. 90–106, doi:10.1016/j.jvolgeores.2015.04.011.

Smith, J., and Wessel, P., 2000, Isostatic consequences of giant landslides on the Hawaiian Ridge: Pure and Applied Geophysics, v. 157, no. 6–8, p. 1097–1114, doi:10.1007/s000240050019.

Staudigel, H., and Schmincke, H., 1984, The Pliocene seamount series of La Palma/Canary Islands: Journal of Geophysical Research–Solid Earth, v. 89, no. B13, p. 11,195–11,215, doi:10.1029/JB089iB13p11195.

Stein, C., and Stein, S., 1992, A model for the global variation in oceanic depth and heat flow with lithospheric age: Nature, v. 359, no. 6391, p. 123–129, doi:10.1038/359123a0.

Storetvedt, K.M., Serralheiro, A., Moreira, M., and Abranches, M.C., 1989, Magnetic structure and evolution of the island of Santa Maria, Azores: Physics of the Earth and Planetary Interiors, v. 58, p. 228–238, doi:10.1016/0031-9201(89)90056-3.

Trippanera, D., Porreca, M., Ruch, J., Pimentel, A., Acocella, V., Pacheco, J., and Salvatore, M., 2014, Relationships between tectonics and magmatism in a transtensive/transform setting: An example from Faial Island (Azores, Portugal): Geological Society of America Bulletin, v. 126, no. 1–2, p. 164–181, doi:10.1130/B30758.1.

Trota, A., 2008, Crustal Deformation Studies in S. Miguel and Terceira Islands (Azores) [Ph.D. thesis]: Ponta Delgada, Universidade dos Açores, 281 p.

Vogt, P., and Jung, W., 2004, The Terceira Rift as hyper-slow, hotspot-dominated oblique spreading axis: A comparison with other slow-spreading plate boundaries: Earth and Planetary Science Letters, v. 218, no. 1–2, p. 77–90, doi:10.1016/S0012-821X(03)00627-7.

Walcott, R., 1970, Flexure of the lithosphere at Hawaii: Tectonophysics, v. 9, no. 5, p. 435–446, doi:10.1016/0040-1951(70)90056-9.

Watts, A., and ten Brink, U., 1989, Crustal structure, flexure, and subsidence history of the Hawaiian Islands: Journal of Geophysical Research–Solid Earth, v. 94, no. B8, p. 10,473–10,500, doi:10.1029/JB094iB08p10473.

White, S.M., Crisp, J.A., and Spera, F.J., 2006, Long-term volumetric eruption rates and magma budgets: Geochemistry Geophysics Geosystems, v. 7, no. 3, p. Q03010, doi:10.1029/2005GC001002.

Wilson, D., Peirce, C., Watts, A., Grevemeyer, I., and Krabbenhoeft, A., 2010, Uplift at lithospheric swells—I: Seismic and gravity constraints on the crust and uppermost mantle structure of the Cape Verde mid-plate swell: Geophysical Journal International, v. 182, no. 2, p. 531–550, doi:10.1111/j.1365-246X.2010.04641.x.

Zbyszewski, G., and Ferreira, O.V., 1960, Carta Geológica de Portugal—Ilha de Santa Maria (Açores): Lisbon, Serviços Geológicos de Portugal, scale 1:50,000.

Zhong, S., and Watts, A., 2002, Constraints on the dynamics of mantle plumes from uplift of the Hawaiian Islands: Earth and Planetary Science Letters, v. 203, no. 1, p. 105–116, doi:10.1016/S0012-821X(02)00845-2.

Science Editor: Bradley S. Singer
Associate Editor: Luca Ferrari

Manuscript Received 22 March 2016
Revised Manuscript Received 10 August 2016
Manuscript Accepted 23 September 2016

Printed in the USA